Human perceptual overestimation of whole body roll tilt in hypergravity

Torin K. Clark, Michael C. Newman, Charles M. Oman, Daniel M. Merfeld and Laurence R. Young

J Neurophysiol 113:2062-2077, 2015. First published 24 December 2014; doi:10.1152/jn.00095.2014

J Neurophysiol 113: 2062–2077, 2015.
First published December 24, 2014; doi:10.1152/jn.00095.2014.

Human perceptual overestimation of whole body roll tilt in hypergravity

Torin K. Clark,[1,2] Michael C. Newman,[3] Charles M. Oman,[1] Daniel M. Merfeld,[4] and Laurence R. Young[1]

[1]*Man Vehicle Laboratory, Department of Aeronautics and Astronautics, Massachusetts Institute of Technology, Cambridge, Massachusetts;* [2]*Charles Stark Draper Laboratory, Incorporated, Cambridge, Massachusetts;* [3]*National Aerospace Training and Research Center, Southampton, Pennsylvania; and* [4]*Jenks Vestibular Physiology Laboratory, Massachusetts Eye and Ear Infirmary, Department of Otology and Laryngology, Harvard Medical School, Boston, Massachusetts*

Submitted 30 January 2014; accepted in final form 22 December 2014

Clark TK, Newman MC, Oman CM, Merfeld DM, Young LR. Human perceptual overestimation of whole body roll tilt in hypergravity. *J Neurophysiol* 113: 2062–2077, 2015. First published December 24, 2014; doi:10.1152/jn.00095.2014.—Hypergravity provides a unique environment to study human perception of orientation. We utilized a long-radius centrifuge to study perception of both static and dynamic whole body roll tilt in hypergravity, across a range of angles, frequencies, and net gravito-inertial levels (referred to as G levels). While studies of static tilt perception in hypergravity have been published, this is the first to measure dynamic tilt perception (i.e., with time-varying canal stimulation) in hypergravity using a continuous matching task. In complete darkness, subjects reported their orientation perception using a haptic task, whereby they attempted to align a hand-held bar with their perceived horizontal. Static roll tilt was overestimated in hypergravity, with more overestimation at larger angles and higher G levels, across the conditions tested (overestimated by ~35% per additional G level, $P < 0.001$). As our primary contribution, we show that dynamic roll tilt was also consistently overestimated in hypergravity ($P < 0.001$) at all angles and frequencies tested, again with more overestimation at higher G levels. The overestimation was similar to that for static tilts at low angular velocities but decreased at higher angular velocities ($P = 0.006$), consistent with semicircular canal sensory integration. To match our findings, we propose a modification to a previous Observer-type canal-otolith interaction model. Specifically, our data were better modeled by including the hypothesis that the central nervous system treats otolith stimulation in the utricular plane differently than stimulation out of the utricular plane. This modified model was able to simulate quantitatively both the static and the dynamic roll tilt overestimation in hypergravity measured experimentally.

roll tilt; orientation perception; human; hypergravity; vestibular

HUMANS NORMALLY PERCEIVE THEIR own orientation relative to gravity by utilizing a combination of several sensory cues, including vestibular, proprioceptive, tactile, and visual. In this study, we totally eliminate visual cues and focus primarily on rotational cues provided by the semicircular canals and gravito-inertial cues provided by the otolith organs as well as other potential contributors (e.g., tactile, somatosensory).

Hypergravity, or an environment of greater than the 1 Earth G normally experienced, provides a unique stimulus for studying vestibular perceptual function. In hypergravity, all graviceptor sensory signals, such as those from the otolith organs, are altered, while the semicircular canal cues are presumed unaffected.

Address for reprint requests and other correspondence: T. K. Clark, Man Vehicle Laboratory, Massachusetts Institute of Technology, 77 Massachusetts Ave. 37-219, Cambridge, MA 02139 (e-mail: tkc@mit.edu).

Previous studies have utilized a short-radius centrifuge to create a hypergravity environment and then subsequently had subjects report their static roll tilt perceptions with a subjective visual vertical (SVV) task (Aubert 1861). With the use of this task, subjective measurements indicated that the subjects overestimated their roll angle in hypergravity when statically tilted (Colenbrander 1963; Correia et al. 1968; Miller and Graybiel 1966; Schöne 1964; Schöne and Parker 1967; Schöne et al. 1967). These perceptual errors in hypergravity contrast with those observed in 1 G, often measured using the SVV task; 1-G errors typically are near veridical for smaller roll tilts but show underestimation for large angles (>60°) (De Vrijer et al. 2009; Kaptein and Van Gisbergen 2006; van Beuzekom and van Gisbergen 2000; Vingerhoets et al. 2008, 2009).

Several more recent investigations have studied hypergravity perception (Chelette et al. 1995; Glasauer and Mittelstaedt 1992; Jarchow et al. 2003; Jia et al. 2002; Merfeld et al. 2001, 2005a) and reported results that are consistent with those reported above. For example, Tribukait and Eiken (2005, 2006a, 2006b, 2012) have completed a series of studies investigating orientation perception during centrifuge spin up. However, studies of perception in sustained hypergravity in the presence of dynamic ca-al stimulation have been rare (Gilson et al. 1973; Guedry and Rupert 1991). One of the challenges of studying dynamic perception in hypergravity is that dynamic out of plane head rotations in a fast spinning environment, such as a short-radius centrifuge, will result in a secondary Coriolis cross-coupled illusion (Graybiel et al. 1960; Guedry and Montague 1961; Melville Jones 1970). (To help minimize any potential confusion, we will use “rotation” throughout only to refer to the roll rotation experienced during the experimental roll tilt stimuli, we will use “spin” or “spun” to refer to the planetary motion of the centrifuge).

To produce a hypergravity environment with limited angular velocity, and thus less cross coupling, a larger radius is required. One technique was to use a high-performance aircraft performing a coordinated turn to create the hypergravity environment (Gilson et al. 1973). Subject made active head tilts within the aircraft and reported illusory motions; however, the reports were qualitative and verbal, so it was not possible to quantify the magnitude or dynamics of the illusion. The authors hypothesized that dynamic tilt perception differs from static tilt perception, suggesting this warrants further study.

This was a primary reason for the experimental studies reported herein. More specifically, using a long-radius centrifuge, we sought to quantify both static and dynamic roll tilt perception in hypergravity. Measures of static roll tilt perception provided data for direct comparison to the dynamic responses. We hypothesized that both static and dynamic roll tilt would be overestimated in hypergravity, with more overestimation at larger angles and higher gravity levels. Furthermore, for dynamic roll tilts, we hypothesized that the amount of overestimation would depend on the angular velocity, or speed, of the rotation due to the contributions of the semicircular canals.

While the otolith organs are the body's only sensors specifically focused on transducing gravito-inertial acceleration, other sensory systems might also contribute. Therefore, we specifically note that our studies, like most others (Colenbrander 1963; Correia et al. 1968; Merfeld et al. 2001; Miller and Graybiel 1966; Schöne 1964; Tribukait and Eiken 2006a), cannot directly distinguish gravito-inertial signals provided by the otolith organs from gravito-inertial signals provided by other somatosensors. However, before proceeding, we note two additional facts that suggest a predominant contribution of the otolith organs. First, data show that fully compensated patients suffering total vestibular loss have tilt thresholds that are on average about twice as big as normal (Valko et al. 2012), demonstrating that the otolith organs have about twice the precision of all other graviceptor cues combined. Second, as will be presented and discussed in detail later, our findings suggest that cues in the utricular plane are emphasized relative to those out of the utricular plane, which suggests a primary vestibular influence on the processing of gravito-inertial cues.

Several mathematical models have been proposed to explain the overestimation of static roll tilt observed in hypergravity. Early on, the utricular shear (Schöne 1964; Schöne and Parker 1967; Schöne et al. 1967) and tangent models (Correia et al. 1968) were proposed to approximate the static overestimation observed in hypergravity by modeling only otolith stimulation. A nonlinear model of otolith function was constructed to predict tilt perception over a range of altered gravity levels and orientations (Dai et al. 1989). More recently, a model was developed to predict static orientation perception in altered gravity environments using otolith and tactile cues (Bortolami et al. 2006b). Mittelstaedt (1983a, 1989, 1986) proposed the concept of an "idiotropic vector," an internal mechanism that drives perceptions in the direction of a person's own longitudinal axis. By incorporating nonlinear otolith transduction (Fernandez and Goldberg 1976b), Mittelstaedt was able to model overestimation in hypergravity.

However, none of these models have attempted to predict hypergravity perception during dynamic tilts, which is a focus of our study. A variety of dynamic models (MacNeilage et al. 2008) have been proposed for 1 G relating the vestibular system to spatial orientation perception employing physiological and mathematical concepts such as Kalman filters (Borah et al. 1988), extended and unscented Kalman filters (Selva 2009), internal models (Green and Angelaki 2004; Merfeld et al. 1999), particle filters (Karmali and Merfeld 2012; Laurens and Droulez 2007), and three-dimensional rotations (Glasauer 1992; Holly et al. 2011; Holly and McCollum 1996). One of these models is based on the "observer" concepts from engineering estimation and control theory (Kalman 1960; Kalman and Bucy 1961; Luenburger 1971) that utilize an internal model of a system to evaluate feedback measurements (Oman 1982, 1990). A comparison of the structure of the Observer model to prior Kalman filter models is provided by Selva and Oman (2012). This family of Observer models (Merfeld et al. 1993; Merfeld and Zupan 2002; Newman 2009; Rader et al. 2009; Vingerhoets et al. 2007, 2009; Zupan et al. 2002) can predict a variety of common illusions using only a small set of free parameters.

However, this family of Observer models does not predict the well-established overestimation in hypergravity, even for static tilts. In fact, at any hypergravity level the Observer model predicts near-veridical perception of static tilt. To our knowledge, a dynamic canal-otolith interaction model has not been proposed that predicts the characteristic overestimation observed for roll tilt perception in hypergravity. We modified this previously proposed, relatively well-validated, dynamic model of orientation perception to mimic the static and dynamic perceptions experimentally observed in hypergravity. As detailed later, we modify the model in accordance with the hypothesis that the central nervous system (CNS) differentially weights otolith signals roughly in the plane of the otoliths' utricular maccule vs. those perpendicular to this plane. We acknowledge that the concept of a "utricular plane" is a considerable simplification since utricular maculae are actually three-dimensional surfaces. However, for simplicity, we consider only the average plane. As discussed later, the saccule is sensitive to gravito-inertial stimulation perpendicular to the principle utricular plane and thus is likely a major contributor to sensing "out of plane" stimulation. Characteristics of afferent neurons for the utricle and saccule appear to differ (Fernandez and Goldberg 1976b), and there is evidence that both contribute to roll tilt perception (Rader et al. 2009), potentially in differing amounts (Mittelstaedt 1983a,b).

METHODS AND MATERIALS

Human subjects reported their perception of static and dynamic roll tilts performed over a range of actual angles and frequencies, performed at 1, 1.5, and 2 Earth Gs. Subjects reported their roll tilt perception using a "haptic indicator," a bar that they could align to the perceived horizontal. They were trained in its use before the experiment. [The perception reporting method we used has previously been referred to as a "somatosensory task" (Park et al. 2006; Wade and Curthoys 1997). However, to more accurately describe it, we follow the lead of Bortolami et al. (2006a, 2006b) and call it a haptic task.] Since roll rotations on the spinning centrifuge nominally produce the well-known Coriolis cross-coupled illusion we attempted to reduce the impact by performing a preexperimental adaptation protocol. Testing took place over 2 days. On the first day, in the following order, the subjects completed the first half of the cross-coupled illusion adaptation, haptic indicator training, and were introduced to hypergravity. The second day consisted of the second half of the cross-coupled illusion adaptation, refresher training on the haptic task, and finally, all of the hypergravity testing sessions.

A previously proposed canal-otolith interaction model for orientation perception (Merfeld et al. 1993; Merfeld and Zupan 2002) was utilized as a starting point for further modification. We modified the model to incorporate the hypothesis that the CNS weights signals in the utricular plane differently than those out of the utricular plane. The one added free parameter was fit to the static tilt perception observed for a 20° tilt in 2 Gs, and then the model predictions were compared with the experimentally observed static and dynamic roll tilt perceptions.

Motion paradigm. Subjects (n = 8) were seated in the cab of the National AeroSpace Training and Research (NASTAR) Center's ATFS-400 long-radius centrifuge facing tangentially towards the direction of travel (see Fig. 1 for motion paradigm). Subjects were restrained with a five-point harness seat-belt. A form-fitting custom head and shoulder support was utilized to restrict roll or yaw head movements and provide support for the torso. Pitch head tilt was also restrained but subjects could actively free their heads in the case of an emergency (e.g., G-force-induced loss of consciousness or vomiting). Vacuum cushions provided broad support across the shoulders and upper arms to broadly distribute tactile cues, and the interior of the cab was dark to eliminate all visual cues. Subjects wore a custom-sized helmet with noise-cancelling headphones to reduce auditory cues from the mechanical systems of the centrifuge. The headphones were also used for communication between the experimenter and the subject. An infrared camera allowed the experimenters to visually monitor the subject during testing.

The centrifuge cab was located on the end of the centrifuge arm (7.62 m). The centrifuge was slowly spun up to the desired gravito-inertial force (GIF) level over 60 s. During the spin-up the cab gradually tilted outwards such that the resultant GIF remained aligned with the body axis of the cab and z-axis of the subject ($+G_Z$). Thus, from the subject's perspective, the direction of the GIF did not change; it only increased in magnitude to create the hypergravity environment. The desired G level was produced at approximately the subject's head level (i.e., within ~5 cm). The gravity gradient along the length of the subject's body was small due to the large radius of the centrifuge and presumably had a minor impact on perception. For a 1.83-m (6 foot) tall seated subject, the maximum gradient achieved for the worst-case 2-G condition was ~0.21 Gs from head to feet and 0.13 Gs from head to buttocks. Once the final G level was reached, a 60-s wait time was provided for the transient effects of the spin-up to subside and to allow for the subjects to become comfortable in the hypergravity environment. Subjects then experienced a series of passive, whole body roll tilts during the testing period. Once complete, the centrifuge was spun-down, also over 60 s. Completion of the spin-up, transient wait, testing period, and spin-down took less than 19 min.

Roll tilt profile. In the hypergravity environment, subjects experienced a series of passive cab rotations. The cab rotated about the subject's body-fixed roll axis (i.e., "x-axis"), with the center of rotation located near the center of the subject's head. Each rotation went from "upright", or aligned with the resultant GIF direction, to a specific final angle (θ_f) at a specific frequency (f). The rotation profile is given in *Eq. 1* and was selected because it has no discontinuities in angular acceleration, velocity, or displacement. There is a step in the derivative of acceleration (i.e., jerk) and higher derivatives.

$$\theta(t) = \theta_f\left(\mathrm{f}t - \frac{1}{2\pi}\sin(2\pi \mathrm{f}t)\right) \text{ where } 0 \le t \le 1/\mathrm{f} \qquad (1)$$

The angles tested were 10, 20, and 40°. All of the rotations were to the subject's left (counterclockwise) except 20°, which was also tested to the right (clockwise). This allowed for the evaluation of the hypothesis that there are no directional asymmetries. Leftward tilts were selected as the primary direction because it tilted the cab back towards Earth vertical, leaving the subjects closer to upright if stopped for an emergency.

The frequencies of the changes in roll tilt were 0.0625, 0.125, and 0.25 Hz (or periods of 16, 8, or 4 s, respectively). The angles and frequencies were selected to span the region where sensory integration between semicircular canal and otolith cues is believed to occur for dynamic roll tilt (0.1–0.2 Hz) in humans (Merfeld et al. 2001, 2005a,b; Zupan et al. 2002). The maximum peak angular velocity, just 20°/s for the combination of 40° at 0.25 Hz, does not yield large Coriolis cross-coupled stimulation, which roughly scales with angular velocity as well as net angular displacement. After the cab tilt was completed, it remained in the resulting orientation for 30 s and then followed the reverse profile back to "upright" with respect to the GIF direction. After another 30-s stationary period at upright, the next roll tilt began. An example complete profile is shown in RESULTS (see Fig. 3).

Independent variables. Each of the 12 roll tilt combinations (3 frequencies × 4 angles) was presented once per session in a randomized order. Subjects remained naïve that either specific roll angles or frequencies were presented, and this was confirmed in posttesting debriefs. The 12 roll tilt combinations within a session were tested at a specific gravity level: either 1, 1.5, and 2 Gs. Each G level was presented twice, for a total of six testing sessions. Subjects were removed from the centrifuge cab and had a break of at least 20 min between sessions. The gravity levels for each session were presented in counterbalanced orders with each gravity level presented in one of the first three sessions and one of the last three sessions.

Dependent variables. During the 12 roll tilts, subjects reported their perceived roll orientation using a horizontal "haptic indicator" (Wade and Curthoys 1997). The horizontal haptic task has been well validated in a variety of other studies, especially those focused on assaying dynamic effects (Merfeld et al. 2001; Park et al. 2006; Rader 2009; Rader et al. 2009, 2011; Wade and Curthoys 1997; Zupan and Merfeld 2003). This task was selected due to several advantages for our specific goals. First, using a haptic task allowed us to totally eliminate all visual cues, which we felt was critical to avoid dynamic visual-vestibular interactions for this quantitative study of dynamic tilt perception in hyper-G. Second, compared with visual techniques (i.e., SVV), haptic responses are not potentially contaminated by torsional eye movements (Betts and Curthoys 1998; Goonetilleke et al. 2008; Wade and Curthoys 1997). This is especially a potential confound in hypergravity where it is well known that ocular counter-rolling is enhanced (Colenbrander 1963; Miller 1962; Miller and Graybiel 1971; Woellner and Graybiel 1959). Third, the SVV task is traditionally used for static roll tilt perception, while one of our foci is to study dynamic perception. Several studies have extended this technique to dynamic tasks using repeated stimuli presented via an adaptive staircase and forced-choice responses (Kaptein and Van Gisbergen 2006; Vingerhoets et al. 2007, 2008). However, this method requires many (>10) presentations, which was not feasible in hypergravity, both for subject comfort, but also because subject responses were likely to adapt with repeated presentations. Fourth, compared with vertical haptic tasks, typically done with a single hand (Barnett-Cowan and Harris 2008; Bauermeister et al. 1964; Borah and Young 1982), fewer left/right asymmetries are likely to occur for a horizontal task due to its symmetric nature. Fifth, compared with other discrete tasks (e.g.,

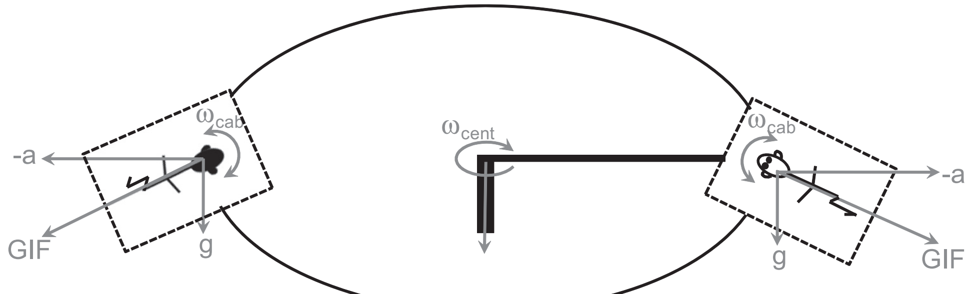

Fig. 1. Schematic of hypergravity motion paradigm in quasiperspective view. The seated subject is inside the closed cab of the centrifuge (dotted box). The centrifuge spins clockwise (ω_{cent}) about an Earth-vertical axis, creating an Earth-horizontal centripetal acceleration (a), which combines with gravity (g) to yield the net gravtio-inertial force (GIF). The cab and subject are then tilted relative to the GIF (ω_{cab}).

verbal reports or "perceptual upright" P vs. d differentiation; Dyde et al. 2006), it is possible to obtain temporally continuous reports.

The indicator consisted of a 30.5-cm long metal bar, which pivoted at its center point and was connected to a potentiometer (Vishay Spectrol 601HE0000B01 Hall Effect Position Sensor) for recording the response. The bar was located ~35 cm from the midriff of the seated subject (Merfeld et al. 2001). Subjects were instructed to hold the indicator at the ends with each hand using their finger tips and were not allowed to move their hands along the length of the bar (Merfeld et al. 2001; Park et al. 2006; Zupan and Merfeld 2003). Subjects attempted to keep the bar aligned with their perceived gravitational-horizontal continuously. At the end of each trial, 10–15 s after returning to upright, subjects performed an "indicator reset," in which they quickly deflected the indicator by at least 40° in each direction several times and then attempted to reset it to horizontal. This action was aimed at making the initial perception for the ensuing trial independent from the final perception of the previous trial. The subject's perceptions were compared with the actual orientation of the cab with respect to the GIF direction, as recorded from the simulator. The haptic indicator only rotated in roll so any perceived pitching or yawing rotation could not be reported.

The experimental design was fully within subjects and complete, such that every subject experienced every combination of roll angle, roll frequency, and gravity level. The repeated-measures design allowed for fewer total subjects, reducing the time spent completing preexperimental protocols. The complete design was necessary to study interactions among independent variables. There were two replications of each treatment level combination to test if adaptation was taking place.

Cross-coupled stimulus adaptation protocol. As previously described, when subjects make head rotations in a spinning environment, such as employed here, they will experience an illusory perception of rotation about an unexpected axis, orthogonal to head roll rotation and centrifuge spin axes. To minimize the impact of the cross-coupled illusion during dynamic rotations on a centrifuge, we utilized both a large radius rotator and a preadaptation protocol (Brown et al. 2002; Cheung et al. 2007; Young et al. 2003) before hypergravity testing on the centrifuge. The following protocol was designed to adapt subjects to this illusion through repeated exposure, such that subjects could effectively report perceptions of roll tilt in hypergravity.

In the dark, upright subjects were passively spun in pure yaw. Subjects repeated a series of four active, head-on-body roll tilts, always in the same order: *1*) from upright to right ear down, *2*) right ear down back to upright, *3*) upright to left ear down, and *4*) left ear down back to upright. The cross-coupled stimulus adaptation protocol consisted of three phases. In the main (chronologically second) phase, the subject was incrementally adapted to the cross-coupled illusion by manipulation of the spin rate. The spin rate began such that the cross-coupled illusion was near threshold. As the subject adapted and the illusion became subthreshold the spin rate was increased slightly. This process was repeated for 15 min, incrementally adapting the subject to the cross-coupled illusion. The threshold-based adaptation technique was advantageous because subjects were only exposed to near threshold level illusions, making it less provocative of motion sickness than other adaptation protocols (Cheung et al. 2007).

In the first and third phases, pre- and postmeasures of the illusion's intensity were taken to measure the adaptation that took place at a fixed yaw rate of 14.26 rpm (the maximum spin rate of the centrifuge in the hypergravity tests). The intensity was reported using the following scale: 0 corresponded to no unusual sensation such as would be experienced during a head tilt in everyday life and a 10 was arbitrarily assigned as the intensity of the first head tilt in the premeasure phase (Brown et al. 2002; Jarchow and Young 2007; Young et al. 2001). For the pre- and postmeasure phases, subjects performed just one series of the four head tilts. The adaptation protocol was performed twice, once the day before the hypergravity testing and again the morning of testing.

The mean illusion intensity across head tilt direction decreased as a result of the adaptation protocol. A two-factor (pre- vs. postmeasure and *day 1* vs. *2*) repeated-measures ANOVA found the mean illusion intensity decreased after each adaptation session [$F(1,7) = 9.6$, $P = 0.018$] and on the second day [$F(1,7) = 37.2$, $P < 0.0005$].

We cannot be certain that the cross-coupled stimulus adaptation protocol could not subsequently impact subjects' perceptions during the experiment; however, there are a number of responses to suspect that any such impact was minimal. First, there is evidence that adaptation to the cross-coupled stimulus is specific to the particular adapted axis (Garrick-Bethell et al. 2008), such that the adaptation to the cross-coupled illusion in pitch would not affect roll tilt perception. Second, 1-G roll tilt perceptions after adaptation were similar to those previously reported. Third, an individual subject's roll tilt perception in hypergravity did not appear to depend on how much cross-coupled adaptation took place.

Training. While the haptic task was quite intuitive, subjects were provided training in 1 G before the hyper-G test sessions to ensure adequate performance. Subjects were trained by reporting their perceived orientation with the haptic indicator during a 60-s, pseudorandom sum-of-sines roll tilt profile in 1 G (i.e., no planetary centrifuge spin) in the dark. The motion consisted of three nonphase-locked frequencies (0.061, 0.134, and 0.278 Hz), each with an amplitude of 15°, for a maximum potential roll angle of 45°. The first 10 and last 5 s of the profile were scaled such that it began and ended at an upright orientation.

Following each trial, subjects received general feedback on performance (e.g., "You reported angles larger than you were exposed to. Try tilting the bar less aggressively."). Quantitative performance scores (e.g., root-mean-square error from upright) were provided intermittently every few trials. Subjects repeated trials until their performance, measured by root-mean-square error, improved to a steady state. Usually 10–18 trials were presented in the primary training session on the first day. On the second day, three to four additional training trials were presented just before testing to ensure performance had not degraded. Responses from these pseudorandom sum-of-sines training trials were fit with a simple input-output model incorporating a bias, gain, and time delay. After training, generally the biases were near 0, the gains near 1, and time delays ranged from 100 to 350 ms. This delay is within the range of previously reported vestibular perception response delays (Barnett-Cowan 2013), despite differences in stimuli utilized and the continuous haptic perceptual task we used.

Finally, before testing, subjects were exposed to hypergravity to help reduce anxiety and expose them to the physiological effects of hypergravity (e.g., increased heart rate). The centrifuge was spun up to 1.5 Gs and then 2 Gs for 2 min each. Transitions between gravity levels were 1 min. During these training sessions, the roll angle of the cab was controlled to always remain aligned with the net GIF.

Subjects. All protocols were approved by the Environmental Tectonics (ETC)/NASTAR Center's Internal Review Board (IRB) and Massachusetts Institute of Technology 's (MIT's) Committee on the Use of Humans as Experimental Subjects (COUHES). Inclusion criteria were defined before the start of the study. Subject inclusion criteria included healthy females and males ages 18–65, with no known vestibular defects or conditions. Subjects who were highly susceptible to motion sickness were excluded from the study, as determined by scoring above the 90th percentile on the Motion Sickness Susceptibility Questionnaire (MSSQ) (Golding 1998, 2006). Individuals with no history of any motion sickness (0th percentile on the MSSQ) may not have a normally functioning vestibular system and thus were also excluded from the study. In addition, subjects completed NASTAR Center's medical screening questionnaire and if a subject responded "YES" to any of the questions, a FAA Class III Physical was required to participate in the experiment. No subject met any exclusion criterion, likely because of self-selection among those who volunteered. All subjects signed a written informed consent form.

Eight subjects were tested (5 males/3 females, ages 21–32 yr, mean = 26, SD = 3.2). Two subjects had minimal flight experience (< 50 h), two had minimal centrifuge experience (< 6 h), and the remainder had no prior flight or centrifuge experience. The subjects with prior experiences did not have results that appeared to differ from the remaining subjects. All subjects were able to complete the protocols and experienced no serious adverse effects. Minor motion sickness symptoms occurred for every subject; however, no subjects approached vomiting nor asked to stop the experiment. Due to technical issues, *subject 1* only completed four sessions (omitting the second 1.5- and 2-G tests) and *subject 2* did not complete the last session at 2 G.

Data analysis. The subjects' perception was analyzed at specific points during the rotation profile. A measure of upright static perception was taken at the beginning of each test session just before any tilt motions. Even when upright with respect to the gravito-inertial cue, subjects were instructed to keep the indicator aligned with their perception of gravitational-horizontal, reporting upright relative to perceived gravity, not upright relative to their body orientation. Subjects performed an "indicator reset" and then aligned the bar with their perceived horizontal. The average response over the 2 s just before the beginning of the first tilt was taken as a measure of upright perception. The metric for static tilt perception was the average haptic indicator response over the 2 s just before the beginning of the dynamic return. This was 28–30 s after the end of dynamic tilt (see Fig. 3). To statistically test the effect of hypergravity on static tilt perception, we used the following hierarchical regression:

$$\left(\theta_{\text{per}} - \theta\right)_{ij} = \rho_i + \beta\left(\left(\text{G} - 1\right)\theta\right) + \epsilon_{ij} \qquad (2)$$

The error in perceived roll in degrees ($\theta_{\text{per}} - \theta$) from the *j*th measurement in the *i*th subject were a function of the "G-Excess" term [(G-1)θ], where G is the gravity level (1, 1.5, or 2 Gs) and θ is actual roll angle in degrees. In addition, the regression has subject-dependent intercepts (i.e., biases; ρ_i, where i = 1–8 subjects). In the first stage of the regression, the subject's random effects are accounted for (ρ_i), accounting for the within-subjects design. In the second stage, the perceptual errors were regressed on the G-Excess term. This analysis is appropriate for the within-subjects design and treats the effects of gravity and angle as linear over the values tested. The "residual" error on the *i*th measurement for the *j*th subject is denoted ϵ_{ij}.

To quantify the perception during dynamic rotations (i.e., tilt or return), a metric was used to compare the perceived roll rotation motion to the actual roll rotation motion. A linear fit was applied to the 50% of the dynamic rotation period that was centered temporally, for both the actual roll rotation and the perceptual response. The slope of the perceptual response (m_{per}) was normalized by the actual slope (m_{act}) and used as the primary metric for the dynamic rotation perception. The metric was selected because it was robust to subject sensorimotor reaction delays and differences in the perceptual response just preceding the dynamic period. From training data, sensorimotor reaction delays were estimated to range from 0.10 to 0.35 s and pretilt errors were generally within ±5° from upright on individual trials. While neither the actual dynamic rotation nor the perceptual responses were linear over the entire dynamic period, over the central 50% both were reasonably approximated as linear. Perceptual responses that had R^2 values <0.75 were rare and were excluded from the analysis (16 of 532 for tilts, and 18 of 532 for returns). A normalized slope metric of unity indicates accurate dynamic perception. Slopes greater than or less than one correspond to overestimation or underestimation, respectively. While the slope metric measures the rate of change of perceived roll tilt, we do not consider it a direct measure of perceived angular velocity. Subjects were instructed to instantaneously match the indicator position with perceived tilt, as opposed to match indicator rotation rate with perceived angular velocity. This is an important nuance since perceived angular velocity and changes in perceived tilt are often dissociated (e.g., perceived tumbling from the cross-coupled illusion without comparable changes in perceived orientation). Dynamic perception can be related to static tilt steady-state perception by comparing the normalized slope metric to a ratio of the static tilt perceived angle to the actual angle.

The normalized slope metric was fit with the hierarchical regression in *Eq. 3*. The regression was designed to test if dynamic perception was effected by G level, if that effect depended on angular velocity, and if that effect changed between the first and second session in a particular hypergravity level. The regression controls for subject, angle/frequency combination, and direction (i.e., tilt vs. return) in the first three terms of *Eq. 3*.

$$\left(\frac{m_{\text{per}}}{m_{\text{act}}}\right)_{\text{ijk}} = \rho_{\text{i}} + \lambda_{\text{j}} + \tau\text{DIR} + \beta\left(\text{G} - 1\right) + \kappa\left(\text{G} - 1\right)\omega_{\text{peak}} + \delta\left(\text{G} > 1\right)\text{REP} + \epsilon_{\text{ijk}} \qquad (3)$$

In *Eq. 3*, ρ_i is the intercept for subject i = 1–8, λ_j is the 1-G response for the jth angle and frequency combination (3 angles × 3 frequencies: j = 1–9), and DIR is the dynamic rotation direction and is either 0 for tilts or 1 for returns. The "residual" error on the *i*th subject, *j*th angle and frequency combination, and *k*th trial is ϵ_{ijk}. The remaining terms all address the effect of hypergravity on the dynamic perceptual response, where G is the gravity level in Gs, ω_{peak} is the magnitude of the peak angular velocity for the rotation, and REP is either 0 for the first session at a particular hypergravity level or 1 for the second session at that hypergravity level. The REP term is only active for hypergravity levels (G > 1). In 1 G this term is omitted, even on the second session, since we expect there to be no adaptation in 1-G responses. In hypergravity, however, we hypothesize that sensory conflict may lead to adaptation or learning. The level of significance for all tests was set to α = 0.05.

Mathematical modeling. We modified the most widely validated canal-otolith interaction model, aiming to mimic the dynamic and static perception observed in hypergravity. Details of the model are published elsewhere (Merfeld et al. 1993; Merfeld and Zupan 2002; Newman 2009), so we provide just a brief summary here. We utilized the vestibular pathways of the most recent version of the model (Newman 2009), which is shown schematically in Fig. 2. In the model, it is assumed that the CNS neural networks have learned the normal relationships between head orientation and motion and the corresponding semicircular canal and otolith afferent responses. These "internal models" compute expected sensory afference signals (e.g., for the canals and otoliths), which are compared with actual afference. The resulting "sensory conflict" errors are weighted by constant scalar feedback gains used to "steer" the perception of orientation to values that minimize the errors. There are five feedback gains which serve as the only free parameters in model and were set according to the values used by Vingerhoets (2007), who validated entirely on perceptual data (Table 1). The model describes perceptions resulting from passive, nonself-generated motions, although the frequency content of active motions typical experienced (e.g., locomotion) presumably influences the model parameters. Finally, it is essential to note that in the integration of estimated angular velocity to yield the estimated gravity vector an internal estimate of the magnitude of gravity is applied. Since the majority of our lives we operate in an environment in which the magnitude of gravity is near 1 G, we assume this internal magnitude is properly calibrated to 1 G.

We hypothesized that the limitation in the vestibular Observer model preventing the expected overestimation in hypergravity was in the otolith pathways. Therefore, the proposed modification was made in the otolith pathway (K_{a} pathway in Fig. 2), while the canal and canal-otolith interaction pathways were left unmodified. We hypothesize that the CNS treats otolith stimulation in the utricular plane differently than that out of the plane (i.e., in the direction perpendicular to the utricular plane). In particular, the relative weighting on the otolith sensory conflict signal is not the same in all directions; signals

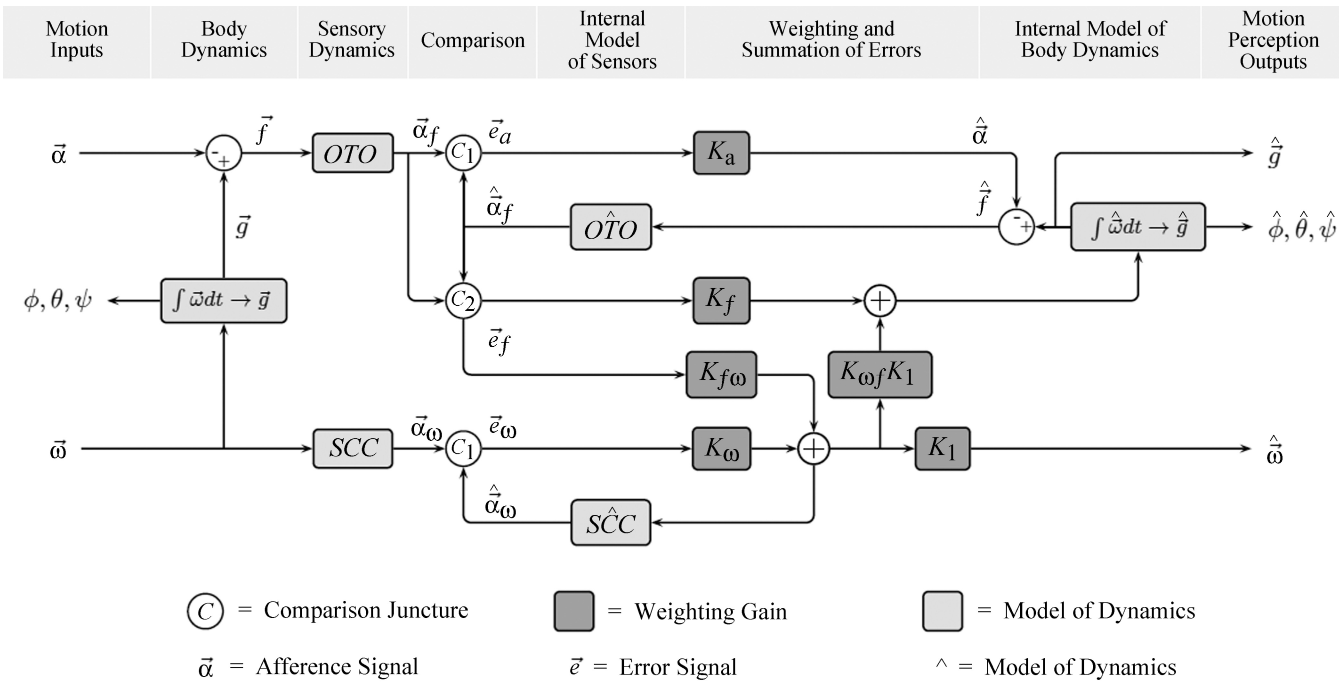

Fig. 2. The vestibular Observer model. The model flows from left to right. On the left the "experimenter" provides actual motion inputs. On the right the model provides predictions of the human perception of those motions. The model functions in a head-fixed right-handed coordinate system such that the *x*-axis aligns with the naso-occipital axis, the *y*-axis aligns with the interaural axis, and the *z*-axis is perpendicular to the *x*- and *y*-axes. The positive direction of the *x*-axis is forward, of the *y*-axis is left, and of the *z*-axis is cranial. All of the vectors in the model are then 3-dimensional, with each component representing the signal along the corresponding [*x*, *y*, *z*] axis. Details on the pathways are in the text. $K_1 = (K_\omega + 1)/K_\omega$.

resulting from the utricular plane are weighted differently than those out of the plane (i.e., in the direction of saccule primary sensitivity). As discussed later, the proposed differential weighting could be related to the differences in the number or sensitivity of utricular vs. saccular afferent neurons or by our roll tilt task that is more sensitive to utricular contributions.

Previous versions of the Observer model (Merfeld et al. 1993; Merfeld and Zupan 2002; Oman 1982, 1991; Rader et al. 2009; Vingerhoets et al. 2007, 2009; Zupan et al. 2002) have all utilized scalar feedback gains, implicitly assuming that rotations around and accelerations along *x*-, *y*-, and *z*-axes are equivalent. Here, we propose using a vector feedback gain, specifically for the linear acceleration feedback (K_a), to allow for different weightings of the linear acceleration sensory conflict error ($\vec{e}_a$) in the utricular plane (K_{a_u}) vs. out of the plane ($K_{a_{u\perp}}$). For simplicity we left the linear acceleration feedback gain on errors out of the utricular plane ($K_{a_{u\perp}}$) at the nominal value of −4.0. The linear acceleration feedback gain on errors in the utricular plane (K_{a_u}) was then adjusted to $K_{a_u} = -2.0$ to best mimic the average static perception observed for one specific hypergravity case (a 20° roll tilt in 2 Gs). Note that this decrease in sensitivity for the acceleration pathways in the utricular plane yields an effective relative increase in sensitivity for the tilt pathways in the utricular plane, since the model interprets otolith cues as being due to either tilt or translation (acceleration).

Table 1. *Modified model residual weighting parameters*

Parameter	Value	Units
K_{a_u}	−2	Unitless
$K_{a_{u\perp}}$	−4	Unitless
K_f	4	1/s
$K_{f\omega}$	8	1/s
K_ω	8	Unitless
$K_{\omega f}$	1	Seconds

The model was implemented in MATLAB-Simulink 2012a (The MathWorks) software suite. The Simulink model was configured with a variable time-step fourth order Runge-Kutta differential Eq. solver (ode45 Dormand-Prince). The model was simulated with the same motion profiles applied from the experiment (Fig. 3), using a 100-Hz sampling rate. Specifically, the roll tilt profile from *Eq. 1* was simulated (see Fig. 3*B*) at different gravity levels. For simulation purposes each desired gravity level was simulated by modifying the magnitude of gravity in the model as opposed to simulating the complex angular velocity and acceleration profiles involved in the centrifugation paradigm. However, we also performed control simulations with the full centrifugation paradigm and found no noticeable impact on roll tilt perception. The static perception can also be calculated as a function of roll tilt angle and gravity level analytically instead of using the full dynamic simulation, albeit a numerical equation solver is required (see APPENDIX for details). To allow direct comparison, static and dynamic perception metrics for the model predictions were calculated as described above for the experimental analysis.

RESULTS

Figure 3*A* shows the subjects' average perceptual report from the haptic indicator during an example roll tilt profile in each gravity level: the 20° roll at 0.125 Hz. Gravity level dramatically altered roll tilt perception. In 1 G, subjects perceived their orientation fairly accurately with only slight delay errors during dynamic tilt, dynamic return, and postreturn responses. However, in 1.5 G, subjects overestimated their roll tilt, both in relation to the actual roll angle and the 1-G perception. The perceptual error was even larger in the 2-G case. Figure 3*B* shows the modified model's predicted perceptions for the same stimuli. As desired, the model predicts a fairly accurate perception of the roll tilt profile in 1 G but yields

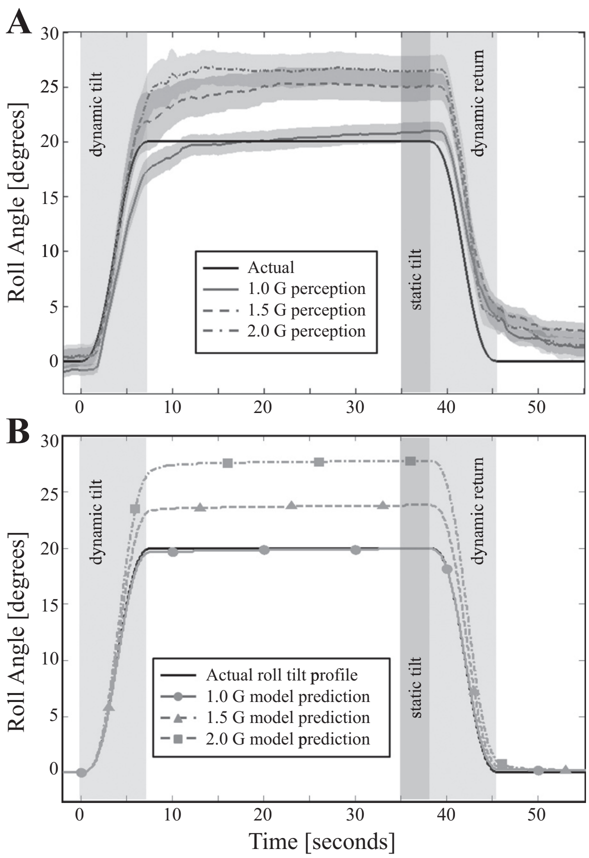

Fig. 3. Roll tilt perception in each gravity level for an example case: 20° roll tilt at 0.125 Hz. *A*: experimental results. The mean across subjects ±1SE is shown. *B*: modified model predictions for the same roll tilt stimuli. The dynamic tilt, static tilt, and dynamic return periods are highlighted.

static and dynamic overestimation in 1.5 and 2 G. The predicted time courses mimic those observed experimentally (Fig. 3*A*) across each gravity level and each phase of the tilt profile.

Upright static perception. A repeated-measures ANOVA with gravity level as the independent variable found there to be no evidence that hypergravity affected upright roll tilt perception ($P = 0.71$). Even in hypergravity, reported roll tilt perception was veridical (i.e., upright when untilted). This is consistent with previous studies using SVV tasks (Colenbrander 1963; Correia et al. 1968; Miller and Graybiel 1966; Schöne 1964; Schöne and Parker 1967; Schöne et al. 1967).

Static tilt perception. The static perception of roll angle is plotted vs. actual roll angle relative to the GIF in Fig. 4*A*. To

Table 2. *Static tilt statistical regression fit*

Coefficient	Units	Estimate	Standard Error	*Z* Value	*P* Value
$\bar{\rho}_i$	Degrees	−0.065	0.82	−0.08	0.94
β	1/Gs	0.35	0.026	13.39	<0.0005

more clearly view the effects of the gravity level, the error in perceived angle (perceived minus actual) is shown in Fig. 4*B*. Here, and throughout, positive errors indicate a perceived roll angle to the left (counterclockwise) of the actual angle and negative errors correspond to the perceived angle being to the right (clockwise) of the actual roll. No evidence was found that static tilt steady-state perception had any learning or adaptation effects (paired *t*-tests comparing the same presentation in session 1–3 to that in session 4–6; $P = 0.39$ for 1 G, $P = 0.23$ for 1.5 G, $P = 0.51$ for 2 G), so the two presentations were pooled. Furthermore, as expected, the static tilt steady-state perception showed no evidence of being dependent on dynamic rotation parameters, particularly the roll frequency ($P = 0.46$). Thus the presentations of specific angle at each of the three frequencies were pooled. Finally, no evidence was found that static tilt steady-state perception had any left/right asymmetries (paired *t*-tests between −20 and 20° tilts; $P = 0.12$ for 1 G, $P = 0.80$ for 1.5 G, and $P = 0.80$ for 2 G).

In 1 G, on average subjects accurately perceived their roll tilt, although the −20° (to the right) roll angle was perceived as slightly (2–3°) greater, or more to the right, than veridical. In 1.5 and 2 G, systematic perceptual errors were seen. Positive (to the left) angles had positive errors and negative angles had negative errors, corresponding to subjects overestimating their roll angle in hypergravity, increasing with G level.

The regression fit in *Eq. 2* was applied to the static tilt perceptions and the results are given in Table 2. The subject intercepts (ρ_i) were found to not be consistently different from zero (*t*-test), further supporting the observation that, when upright, subjects accurately perceive themselves as upright, even in hypergravity. The significantly positive β-coefficient supports the hypotheses that *1*) hypergravity causes overestimation of roll angle, *2*) there is more overestimation at greater hypergravity levels, and *3*) there is more overestimation in hypergravity at larger roll angles. In hypergravity, the perceptual errors in roll tilt were substantial; across the angles tested, the regression indicates that the overestimation was ~17% of the actual roll angle in 1.5 G and 35% in 2 G.

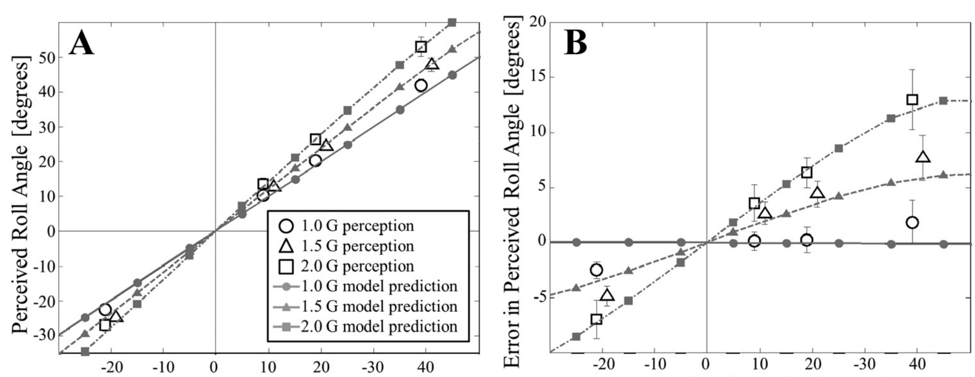

Fig. 4. Perceived roll angle (*A*) and error in perceived roll angle (*B*) across gravity levels. Error is the perceived minus the actual roll angle. The mean across subjects ±1SE is shown. Data points are adjusted along the *x*-axis so as to not overlap; however, all conditions were at −20, 10, 20, or 40° of actual tilt. The modified model predictions are overlaid and match the static overestimation experimental observed in hypergravity across the range of conditions tested.

The modified model was simulated across the same range of roll tilt angles and hypergravity levels as tested experimentally. The model predicted static tilt perception (as above, calculated as the mean perception from 28–30 s after the end of the rotation) was directly compared with that measured experimentally. Even though the added free parameters were selected to fit only a single combination of angle and hypergravity level (20° and 2 Gs), the modified model produced appropriate static perceptual responses (Fig. 4) across each of the combinations of angles and gravity levels tested.

Dynamic tilt perception. We hypothesized that the amount of overestimation in hypergravity during dynamic tilt and dynamic return would be dependent on the roll rotation rate, specifically the peak angular velocity. There was no evidence for left/right asymmetries in the dynamic perception and thus the −20 and 20° cases were pooled. Figure 5 shows the dynamic perceptions (tilts and returns combined) as a function of gravity level for each of the angle and frequency combinations tested. Recall from *Eq. 2* and Table 2 that in 1-G static tilts were, on average, perceived accurately (normalized perception not significantly different from 1), in 1.5 G there was ~17% overestimation (normalized perception = 1.17) and in 2 G there was ~35% overestimation (normalized perception = 1.35). These benchmarks of static steady-state tilt perception are overlaid on the dynamic perception data for comparison.

The positive trend in dynamic perception with increasing gravity level, shown in each tile of Fig. 5, corresponds to overestimation in hypergravity that was greater at higher gravity levels. However, the proportional effect of gravity was not the same for every combination of angle and frequency. At small angles and lower frequencies, corresponding to low peak angular velocities (Fig. 5, *top left*, *A*, *B*, and *D*), the trend with increasing gravity was very steep. At 10° and 0.0625 Hz (Fig. 5*A*), the trend is more extreme than for the static steady-state perception (shown via the horizontal lines). Yet, at larger angles and higher frequencies (Fig. 5, *bottom right*, *I*, *H*, and *F*), the effect of G level on perceived dynamic tilt was much smaller and was clearly less than the normalized static overestimation. To statistically test this, the hierarchical regression fit from *Eq. 3* was applied and the results are given in Table 3.

Table 3. *Dynamic tilt statistical regression fit*

Coefficient	Units	Estimate	Standard Error	*Z* Value	*P* Value
$\bar{\rho}_1$	Unitless	0.90			
τ	Unitless	0.157	0.024	−6.64	<0.0005
β	1/Gs	0.45	0.050	8.91	<0.0005
κ	1/(G × deg/s)	−0.016	0.006	−2.76	0.006
δ	1/Gs	−0.065	0.029	−2.26	0.024

The significantly positive β and significantly negative κ coefficients indicate that *1*) there was significant dynamic tilt overestimation in hypergravity, *2*) there was more overestimation at higher gravity levels, and *3*) the amount of overestimation depended on the angular velocity of the roll rotation. In particular, there was more overestimation at lower angular velocities and less at higher angular velocities. The significantly negative δ-coefficient indicates that on the second repetition of a particular hypergravity level subjects adapted and overestimated the dynamic rotation a little less than on the first repetition. Finally, in all cases, the magnitude of the slope of dynamic returns was perceived as slightly larger than dynamic tilts. However, the effects of hypergravity, angular velocity, and adaptation were similar for tilts and returns.

To visualize the dynamic perceptual response in hypergravity and the dependence on angular velocity, Fig. 6 shows the data for just dynamic tilts in the first session of each gravity level (no adaptation effect). In 1 G, the dynamic tilt perception is fairly consistent across each angular velocity level tested. In hypergravity, there is overestimation in dynamic tilt perception, with less overestimation at higher angular velocities. At low angular velocities, the dynamic tilt perception approaches

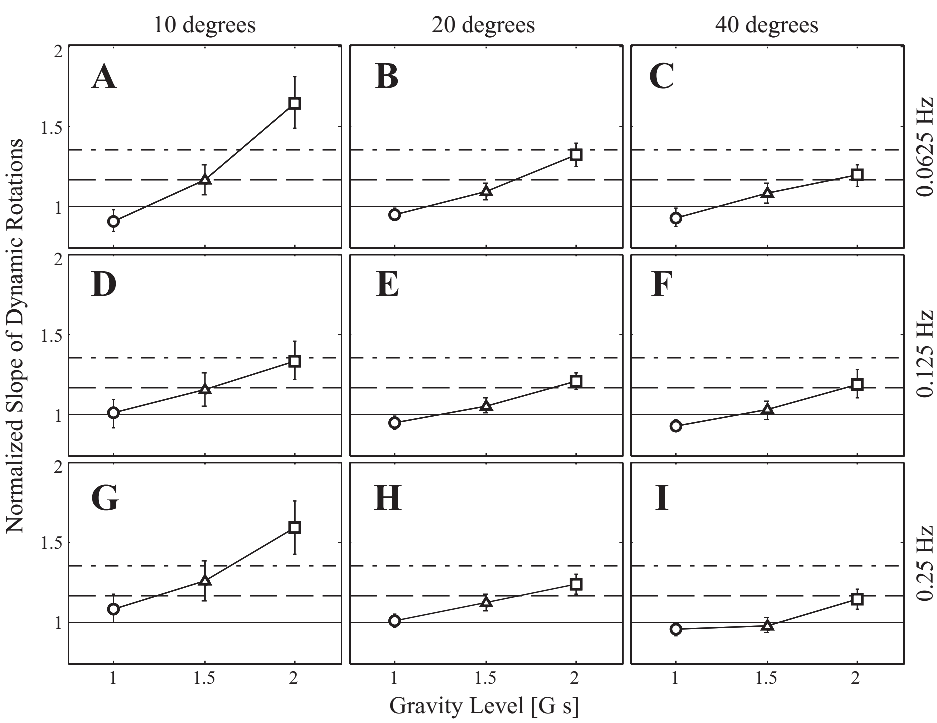

Fig. 5. Dynamic rotation perception as a function of gravity level by angle and frequency. *A*–*I*: 1 combination of angle and frequency. For comparison, the mean normalized static tilt perception is shown for 1 G (solid line), 1.5 G (dashed line), and 2 G (dot-dashed line).

the amount of overestimation observed for static tilts in hypergravity. Perception during dynamic returns and for the second repetition in hypergravity exhibited the same characteristic dependence on angular velocity in hypergravity (not shown graphically) as that in Fig. 6 for the first repetition of dynamic tilts.

Modeling dynamic tilt perception. For the Observer model modifications to be relevant, the model must also be able to simulate the experimental perceptions observed during dynamic rotation. To evaluate the model, it was simulated with the same roll tilt profiles utilized at 1, 1.5, and 2 Gs. The peak roll tilt angle was held constant at 10°, and the dynamic rotation frequency was varied between 0.0625 and 1 Hz to match the peak angular velocities tested (1.25, 2.5, 5, 10, and 20°/s). To allow for direct comparison, the same metric was utilized to quantify the dynamic rotation perception as was employed for the previous experiment: the slope of a linear fit of the simulated perceived roll angle over the central 50% of the dynamic rotation period normalized by that for the actual roll angle. For each simulation, this metric was calculated specifically for dynamic tilts and compared with the mean experimental perception for the first repetition of dynamic tilts, as seen in Fig. 6. For comparison, we also include the model's prediction for normalized static perception (e.g., perceived angle/actual angle) at each gravity level (gray lines in Fig. 6).

The modifications to the model allowed it to produce the characteristic responses of dynamic tilt perception in hypergravity. Specifically, the model predictions matched the experimental perceptions in terms of *1*) near accurate perceptions in 1 G independent of angular velocity, *2*) overestimation in hypergravity with more overestimation at higher gravity levels, *3*) a characteristic dependence of overestimation in hypergravity on angular velocity, with less overestimation at higher angular velocities, and *4*) across all dynamic conditions, less overestimation than static tilts. The comparison of experimental perceptions and model predictions for dynamic returns were qualitatively similar (not shown).

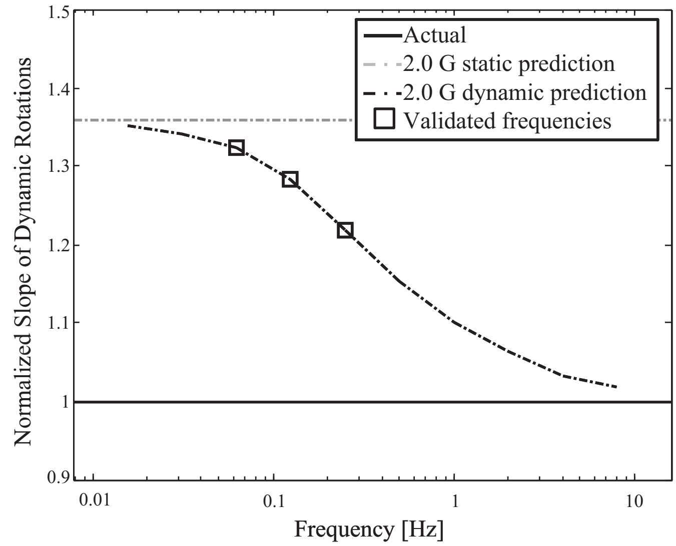

Fig. 7. Modified model prediction of dynamic roll tilt perceptions in hypergravity across a range of frequencies. Predicted dynamic perceptions in 2 Gs (black dashed-dotted line) are compared with predicted static perceptions in 2 Gs (grey dashed-dotted line) and the actual roll tilt (solid black line). The frequencies previously experimentally tested are marked (squares). All simulations were for a 10° roll tilt.

In Fig. 6, the modified model's dynamic perceptions were validated against experimental measures at frequencies of 0.0625, 0.125, and 0.25 Hz in hypergravity. However, the model can be simulated at a much wider range of conditions to more fully understand its predictions. For example, in Fig. 7 it was simulated for a 10° roll tilt in 2.0 Gs at frequencies ranging over 500-fold, from 0.015625 to 8 Hz. The same metric was utilized (i.e., the ratio of perceived slope to actual slope for linear fits over the central 50% of the rotation period) and

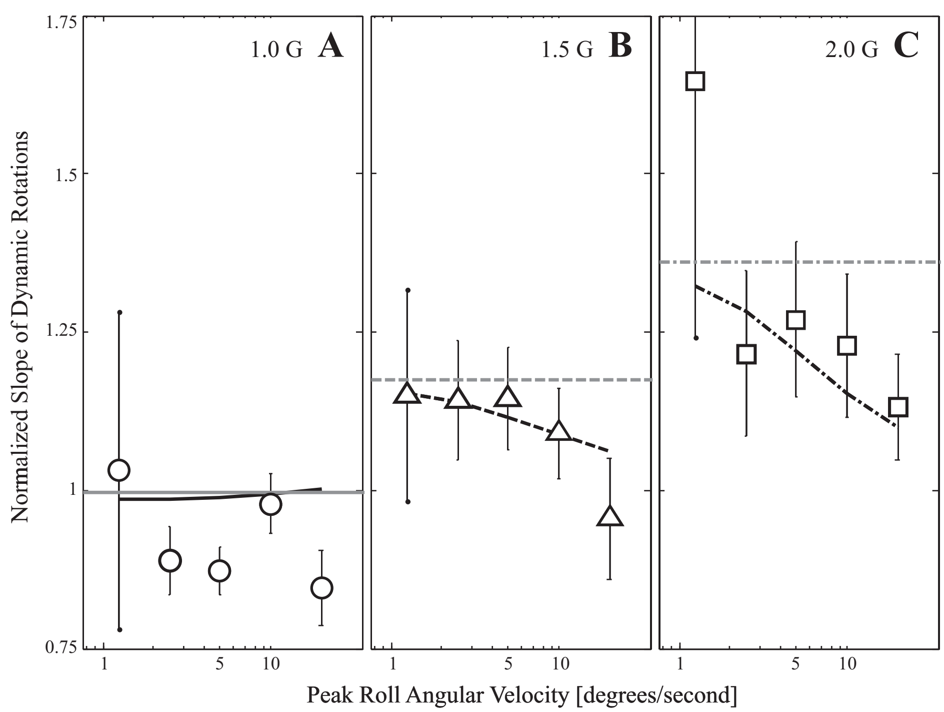

Fig. 6. Dynamic tilt perception as a function of angular velocity by gravity level. *A–C*: 1 gravity level: 1.0 G (*A*), 1.5 G (*B*), and 2.0 G (*C*). The mean data ±1SE are shown. The modified model prediction for dynamic perception is overlaid in black. The modified model prediction for static perception is shown in gray.

compared with the static overestimation from the model and the actual tilt.

As seen in Fig. 7, the modified model predicts that the amount of dynamic overestimation in hypergravity varies substantially across frequencies. As expected, at very low frequencies (<0.05 Hz), the predicted dynamic overestimation approaches the static level. At high frequencies (>5 Hz) the dynamic perception, even in 2 Gs, approaches the actual motion profile (i.e., no overestimation). At middle frequencies, there is a characteristic dependence of the amount of dynamic overestimation inversely depending on frequency. These predictions are consistent with the hypothesis of sensory integration: the CNS combines information from various sensory sources, weighting them by how useful each cue is. The semicircular canal cue is presumed unaffected by altered gravity but does not provide a veridical measure of angular velocity at lower frequencies. The canal information is veridical at higher frequencies and should therefore be weighted more heavily relative to otolith signals, reducing the amount of overestimation in hypergravity. A similar dependence on frequency can be seen in dynamic tilt perception in 1.5 Gs (not shown).

DISCUSSION

We characterized and quantified subject perceptions of static and dynamic whole body roll tilt orientation in 1-, 1.5-, and 2-G environments across a wide range of tilt angles and frequencies. Static roll tilts in hypergravity were overestimated. This finding confirms previous reports (Colenbrander 1963; Correia et al. 1968; Miller and Graybiel 1966; Schöne 1964) but is now supported by statistical analyses. Our study is the first to use a haptic task for indication of the subjective horizontal, whereas previous experiments used an SVV task. The close comparison between measures using the two techniques helps validate our haptic task, which was essential for the dynamic measures that form the focus of this study. For the first time, we quantified dynamic roll tilt perception and found it was also overestimated in hypergravity, with less overestimation at higher angular velocities. We proposed a novel modification to a previous Observer-type dynamic spatial orientation model to allow it to predict the overestimation in roll tilt perception we experimentally quantified. The modification was based on the hypothesis that the CNS treats otolith stimulation in the utricular plane differently than that out of plane. The modified model quantitatively matched the static and dynamic perceptions across the range of gravity levels, roll tilts, and angular velocities that we studied.

Upright static perception. We characterized and quantified subject perceptions of static and dynamic whole body roll tilt orientation in 1-, 1.5-, and 2-G environments across a wide range of tilt angles and frequencies. Confirming previous results, when initially upright, subjects perceived themselves as near upright in roll tilt, even in hypergravity. Accurate roll tilt perception in hypergravity has been previously attributed by the utricular shear theory to the average plane of the utricles being aligned with the Earth horizontal in roll (Corvera et al. 1958; Curthoys et al. 1999; Schöne 1964). Thus when the head is upright (no roll tilt), there is no additional interaural shear force acting on the otolithic membrane of the utricles when the gravity level is increased. While the current experiment was not designed to test this hypothesis, our perceptual data are consistent with it.

There is some evidence of a small leftward bias (3–5°) in roll tilt perception in 1 G using SVV, "perceptual upright," subjective saccadic vertical, and even vertical haptic tasks (Barnett-Cowan and Harris 2008; Barnett-Cowan et al. 2013; Dyde et al. 2006, 2009). However, our data suggest that if this leftward bias exists when using the horizontal haptic task it is <1° or it would have been statistically identified. It is possible the symmetric, two-handed task we utilized reduces the biases observed in a one-handed, vertical haptic task, which may depend on which handed is used (Bauermeister et al. 1964).

Static tilt perception. During static tilt subjects misperceived their orientation in hypergravity. Specifically, subjects overestimated their roll tilt, with more overestimation at higher gravity levels and larger angles. At 1.5 G, the static roll angle was overestimated by ~17% of the actual roll angle, while at 2 Gs it was overestimated by 35%. The proportional effects of angle and gravity level should only be applied at the range of angles and gravity levels tested (i.e., ≤40° and 1–2 Gs). Prior data (Colenbrander 1963; Correia et al. 1968; Miller and Graybiel 1966; Schöne 1964), which match the current data well at up to the 40° angles tested, indicate that at angles larger than ~45° the amount of overestimation begins to decrease with increasing angle. Furthermore, while few studies have tested gravity levels much >2 G, we would hypothesize that at more extreme gravity levels the amount of overestimation would be less than proportional to gravity level. In monkeys, at gravity levels greater than ~4 Gs, the otolith afferent firing rate for some neurons reaches a limit and no longer behaves near linearly with changes in GIF stimulation (Fernandez and Goldberg 1976a,b,c).

As in previous studies (Correia et al. 1968; Schöne 1964), we suspect the overestimation of static roll tilt observed in hypergravity is primarily due to increased stimulation of the utricular otolith organs. However, there are other sensory cues that are likely to be affected by hypergravity and may influence perception. Tactile cues are likely greater in hypergravity. We attempted to distribute tactile cues as evenly as possible (hence minimizing their impact) via body-fitting vacuum cushions. In addition, graviceptive somatosensory cues are likely to be affected by the hypergravity environment. Unfortunately our study, like most others previously (Chelette 2001; Correia et al. 1968; Gilson et al. 1973; Guedry and Rupert 1991; Jia et al. 2002; Miller and Graybiel 1966; Schöne 1964), is unable to differentially stimulate the otolith sensors from the somatosensory cues. Thus the role of the somatosensory information in overestimation of static roll tilt in hypergravity remains uncertain. In one set of studies (Mittelstaedt 1983a; Mittelstaedt and Fricke 1988), a short-radius centrifuge was used to create a gravity gradient along the subject's body, allowing for the differential stimulation of the otolith organs in the head and somatosensory cues in the body. However, this paradigm by design provides a substantive gravity gradient. In contrast, given our goals, we minimized gravity gradients by utilizing a long-radius centrifuge. One study (Miller and Graybiel 1966) utilized labyrinthine-defective subjects (presumably without full otolith function, but with somatosensory information) and found highly variable roll tilt perceptions in hypergravity that did not follow the characteristic overestimation observed in normal subjects. Furthermore, total vestibular loss patients exhibit tilt thresholds about twice as high as normal (Valko et al. 2012) suggesting the otolith organs are the dominate contributors to tilt perception in the dark. This tentatively suggests the critical role of the otolith organs but does not rule out the influence of somatosensory or tactile cues.

The modified model was simulated and found to match the experimental results for static tilts. In particular, static roll tilt perception was predicted over the range of angles and gravity levels tested herein. While the added free parameter was fit to the data in one static tilt condition (20° tilt in 2 Gs), the fact the model mimicked the experimental static tilt results across the range of conditions tested suggests more generalized functionality.

While our primary interest was in hypergravity perception, as a control we also measured roll tilt perception in 1 G. These perceptions are traditionally characterized by slight overestimations for small angles and then underestimation for very large angles (i.e., at least >60°), commonly referred to as E and A effects, respectively (Aubert 1861; Muller 1916). Our 1-G perceptions are near accurate and thus do not appear to exhibit these phenomena. However, we tested at relatively small angles where these effects would be small and difficult to observe. Furthermore, A and E effects have been primarily studied using the SVV (De Vrijer et al. 2009; van Beuzekom and van Gisbergen 2000; Vingerhoets et al. 2008, 2009), whereas we used a haptic task, which may not have these same systematic errors in 1 G (Schuler et al. 2010). A and E effects have been observed using the vertical version of the haptic task (i.e., the subjective tactile vertical), but the results are inconsistent across studies (Barnett-Cowan and Harris 2008; Bauermeister et al. 1964; Bortolami et al. 2006b; Guerraz et al. 2000; Schuler et al. 2010) and the effects are small (~3° peak) at the angles we tested. For the horizontal haptic task we employed, there is not clear evidence for systematic errors in 1 G (Merfeld et al. 2001; Park et al. 2006; Rader 2009; Rader et al. 2009, 2011).

The modified model also does not produce large A- and E-effect perceptual errors in 1 G, which may be considered a weakness. First, as discussed above, these errors are typically only seen using the SVV methodology and are inconsistent or nonexistent when using a haptic task (Barnett-Cowan and Harris 2008; Bauermeister et al. 1964; Guerraz et al. 2000; Schuler et al. 2010). Second, we note that all previous versions of the Observer model also did not produce substantial 1-G errors in roll tilt perception (Haslwanter et al. 2000; Merfeld et al. 1993; Merfeld and Zupan 2002; Vingerhoets et al. 2007, 2008; Zupan et al. 2002), and the modification proposed herein was aimed solely at extending the model to mimic hypergravity perception. Finally, since the perceptual reports we observed in 1 G were near accurate, the model predictions were consistent with the current dataset.

Dynamic tilt perception. As the primary focus of this study, we quantified dynamic roll tilt perception in hypergravity. Perceptual overestimation was also seen during dynamic tilts and returns in hypergravity. The amount of overestimation was generally less than during static rotations; however, overestimation persisted across all angles and frequencies tested. The magnitude depended on the angular velocity of the rotation; at lower angular velocities relatively more overestimation was observed than at higher angular velocities. In particular, at low angular velocities the amount of overestimation tended to approach that observed for static tilts. The angular velocity dependence of the hypergravity effect on perception is supportive of the CNS integrating otolith and semicircular canal sensory sources. The hypergravity paradigm affects the otolith signal but presumably has little or no influence on the canal information. However, it is well known that the canal transduction of angular velocity is bandwidth limited, specifically at lower frequencies or angular velocities (Goldberg and Fernandez 1971). Canal-otolith sensory integration is presumably aware of this canal limitation, and the relative weighting within the integration process is thus dependent on rotation angular velocity (Kaptein and Van Gisbergen 2006; Park et al. 2006). Thus less overestimation in hypergravity at higher rotation rates is consistent with the CNS increasing the relative weighting on the canal signal as transduction improves. This canal-otolith integration, dependent on tilt angular velocity (or frequency if the tilt angle is constant), has been previously observed in 1-G testing paradigms (Angelaki et al. 1999; Park et al. 2006; Vingerhoets et al. 2007; Zupan et al. 2000). The hypergravity paradigm is convenient for testing canal-otolith sensory integration because, as the gravity level is increased, the otolith cue is modulated while the canal information is presumably unaffected. This creates a canal-otolith sensory conflict, and the resulting perception indicates the CNS's weighting of the two conflicting cues.

Effect of cross-coupled stimulus and adaptation. In this set of experiments, the hypergravity environment was created using a centrifuge. While practical for studying hypergravity, the methodology comes with a cost. The spinning environment of the centrifuge causes a secondary illusory perception, the Coriolis cross-coupled stimulus, when any rotations out of planetary spin plane are made. In our centrifuge motion paradigm, the roll tilts utilized will cause a cross-coupled illusion during the planetary spin necessary to create hypergravity. This secondary cross-coupled illusion is separate from the primary hypergravity induced misperceptions and would not occur in a "pure" hypergravity environment such as would be experienced on a more massive planet or approximated in an aircraft making a very large radius constant bank angle turn.

We took several measures to reduce the intensity of the secondary cross-coupled illusion. The illusion's intensity is roughly proportional to the planetary spin rate, roll angular velocity, and net roll displacement of a tilt. To reduce the planetary spin rate for a desired hypergravity level, a long-radius centrifuge was utilized. The roll angles and frequencies selected were selected to remain within reasonable bounds. Furthermore, a preexperimental cross-coupled adaptation protocol was implemented (Cheung et al. 2007) to reduce the subjects' motion sickness and illusion intensities. Despite all of these efforts, the cross-coupled illusion still occurred on at least one roll tilt trial in hypergravity for five of the eight subjects. The illusion occurred significantly more often at higher gravity levels and faster angular velocities, so it may have acted as a confounding factor.

However, the illusion intensities reported, even in hypergravity, were generally very low. Furthermore, data from the three subjects who did not perceive cross-coupling did not appear to differ from data from the five subjects who did report small cross-coupling effects. In addition, it should be noted that the cross-coupled stimulus in our paradigm provoked an illusory pitching sensation, while the hypergravity-induced overestimation of interest was in roll. Subjects were only able to report their roll tilt perceptions using the haptic indicator. The cross-coupled illusion from roll tilt to the right vs. left would be in opposite pitch directions and thus if it significantly influenced dynamic roll tilt perception might lead to a left vs. right asymmetry. However, this was not observed, further suggesting roll tilt was not impacted by the Coriolis cross-coupled illusion. The only way to verify that the secondary cross-coupled stimulus issue did not impact hypergravity perception is to repeat the experiments in a nonspinning environment. For example, a high-performance aircraft performing a coordinated turn could create hypergravity environments at such a low planetary angular velocity that the cross-coupled illusion would be subthreshold.

Adaptation in perceptual responses. Evidence of adaptation in the subjects' perceptual response in hypergravity was identified for dynamic rotations but not static tilts. During testing, there was no feedback provided by the experimenters to help drive this adaptation. Sustained sensory conflict between expected and actual afferent signals, as experienced in hypergravity, is well known to drive sensorimotor adaptation (Bos and Bles 2004; Edgerton et al. 2001; Gonshor and Melvill Jones 1971; Kornheiser 1976; Lackner and DiZio 2003, 2005; Nooij et al. 2008; Oman et al. 1980, 1986; Pettorossi et al. 2013; Reason 1978; Reason and Benson 1978; Seidler 2005; Welch et al. 1998). While sensory conflict probably existed for static tilts in hypergravity, there was not significant evidence of adaptation either in repetitions between sessions or within a session. The passive rotations and the lack of strong feedback from a secondary veridical sensory source may have limited adaptation. Studying adaptation was not the primary purpose of the current experiment so only two presentations of each stimulus were repeated. Additional or longer sessions in hypergravity may result in significant perceptual adaptation for static tilts in hypergravity.

On the other hand, there was evidence for adaptation in hypergravity for dynamic rotations. During dynamic rotation there is feedback on the gravity-influenced otolith signal from the semicircular canals. While the rotations were still passive, the canal signal may have helped drive adaptation more quickly than for static tilts. Only two sessions were presented for each gravity level so it remains uncertain how dynamic perceptual errors in hypergravity may continue to adapt. We hypothesize that with additional sessions the dynamic perceptual errors in hypergravity would continue to decay towards veridical responses.

Modeling dynamic tilt perception. Model simulations of dynamic roll perception showed the characteristic dependence of the amount of overestimation in hypergravity on the angular rotation rate. This is an important contribution because alternative previously proposed models (Bortolami et al. 2006b; Correia et al. 1968; Mittelstaedt 1983a; Ormsby and Young 1976; Schöne 1964) for hypergravity perception only simulate static tilt perception. The currently proposed model is the first to fit dynamic tilt perception in hypergravity or any altered gravity environment. However, one point of difference between the model predictions and experimental perceptions was in 1-G perception. The experimental dynamic tilt perception was on average ~90% of the actual roll tilt slope, and while the model predicts normalized dynamic tilt slopes of slightly less than one, the predicted perception was nearly 98% of the actual roll tilt slope (Fig. 6). This difference may be explained by the human sensorimotor response time delay, which affected the experimental responses but was absent in the simulation.

Dynamic roll tilt in hypergravity was simulated across a wide range of frequencies, beyond those tested herein. The amount of overestimation had strong frequency dependence. Consistent with the concept of sensory integration, the amount of overestimation was reduced at higher frequencies. At very low frequencies (<0.05 Hz), the predicted overestimation approaches the static level, while at high frequencies (>5 Hz), where the canal cues dominate, the tilt perception approaches the actual rotation profile. Other well-validated 1-G dynamic vestibular motion paradigms, including earth vertical yaw rotation, linear acceleration, off vertical axis rotation, and postrotation tilt, were relatively unaffected by the model modifications (simulations not shown).

Implications of the model modification. The modification is based on the hypothesis that the linear acceleration feedback error is weighted differently in and out of the utricular plane. The difference in weighting could be due to a difference in the quality and characteristics of the otolith signals in and out of the utricular plane. For example, the resting discharge rate and sensitivity of otolith neurons from the superior nerve (mainly innervating the utricle) are slightly greater than those from the inferior nerve (mainly innervating the sacculus, which includes a component perpendicular to the utricle) (Fernandez and Goldberg 1976b). Given the differences in the characteristics of the otolith neuron signals approximately within and normal to the utricular plane, it is reasonable to hypothesize that the CNS might weight them differently. As to how the CNS differentiates between in and out of utricular plane stimulation, we can only speculate. Presumably, the CNS develops an understanding of the directional polarization vector of each otolith neuron to facilitate its interpretation. In addition, the CNS may interpret the superior nerve (mainly innervating the utricle) information and inferior nerve (mainly innervating the sacculus) information differently. Alternatively, for roll tilt the CNS may more heavily weight the neurons that are most sensitive for tilts about upright (i.e., those in the y-axis). The precise mechanism of how the apparent differential weighting occurs will require further investigation.

Instead of the difference being in the utricular plane, one could hypothesize that the difference in CNS processing occurs between the head horizontal (x–y) plane and vertical directions. The current experiment focused exclusively on whole body roll tilt perception in hypergravity and thus cannot distinguish the head-horizontal hypothesis from the utricular plane hypothesis (since head y-direction and the utricular plane y'-direction are aligned). However, hypergravity pitch experiments do not support the head horizontal vs. head vertical hypothesis (Cohen 1973; Correia et al. 1968), where at orientations <30° pitched forward (i.e., nose down), increasing hypergravity levels cause subjects to perceive themselves being pitched nose up. These results suggest the importance of the utricular plane since only when pitched forward by 30°, aligning the utricular plane with the increasing GIF, does gravity level not have an effect on perception. The two independent data sets are in close agreement and another study shows a similar effect of hypergravity on static pitch perception (Schöne 1964), which increases confidence in the utricular plane hypothesis. In Correia et al. (1968) and Schöne (1964), whole body tilts were performed, while in Cohen (1973) the tilts were head-on-body suggesting that proprioception in the neck is not the primary cause of the pitch perception asymmetry in hypergravity.

The concept of differential processing of otolith signals in the utricular vs. the saccular plane has previously been proposed. The utricular shear model (Schöne 1964), effectively assumes that stimulation out of the utricular plane is ignored for orientation perception (i.e., weighted by zero). Mittelstaedt (1983a) proposed stimulation in the saccular direction is weighted 54% as much as stimulation in the *y*-axis (utricular shear for roll tilt) direction. Ormsby and Young's model (1976) contained nonlinear treatment of signals depending on their orientation relative to the utricular and saccular directions. Finally, differential weighting has been applied in modeling to roll vs. pitch and yaw angular velocity integration (Glasauer and Brandt 2007). Our modified Observer model builds on these concepts in two distinct ways: *1*) our differential weighting between in and out of utricular plane is done to the otolith acceleration feedback error, not directly to the transduced afferent signal (Mittelstaedt 1983a), and *2*) the differential weighting is done within the framework of a dynamic canal-otolith interaction model, providing dynamic as well as static perception predictions in hypergravity.

Limitations of the model modification. While the modifications within the model are able to explain a wide range of hypergravity perceptual responses, there are still limitations. Our modified version, as well as previous Observer models (Merfeld et al. 1993; Merfeld and Zupan 2002), predict illusory linear acceleration in hypergravity that was not reported by subjects in terms of illusory sensations of linear movement. The predicted illusory response in hypergravity is caused by the internal model of body dynamics representing the physical relationship between gravity, acceleration, and GIF ($\hat{\vec{f}} = \hat{\vec{g}} - \hat{\vec{a}}$). Since the internal estimate of gravity is assumed to have a magnitude of 1 G, the excess internal estimate of GIF is attributed to acceleration. Even when the subject is simply upright in a hypergravity environment, the model predicts an illusory perception of vertical acceleration upward, both in the modified and unmodified versions. The internal estimate of the magnitude of gravity being 1 G is essential to the model mimicking overestimation in hypergravity. If in a 2-G simulation for example, the internal magnitude of gravity is adjusted to 2 G as well, the model will no longer predict illusory acceleration, but it also will not predict the expected overestimation.

There are several potential explanations for why experimental subjects did not report illusory translation associated with the predicted acceleration. First, subjects were presumably aware of the motion capabilities of the centrifuge device. Knowledge or expectation that the centrifuge cab cannot enact translations may quench these sensations that may have existed for an unbiased observer (Wertheim et al. 2001). Furthermore, other nonvestibular cues (e.g., proprioceptive, tactile, and somatosensory) may have helped quench illusory translation percepts. We did not attempt to model either the subjects' expectation of the device's feasible motions nor nonvestibular pathways. There is evidence (Merfeld et al. 2001) that during centrifugation when the subject's precept of orientation is not aligned with the GIF (as is the case during roll tilt in hypergravity), horizontal vestibular ocular reflex (VOR) eye movements do occur. The horizontal VOR would correspond to the horizontal linear acceleration observed in the model simulations. An expectation in feasible motions or integration of nonvestibular cues could both explain the divergence between reported perceptions and the VOR response.

Other nonotolith graviceptor (e.g., somatosensory) sensors are likely to be influenced by hypergravity. However, we did not attempt to include them in the model since our experimental hypergravity paradigm is unable to differentiate between otolith and extra-otolith graviceptors. Future modeling efforts will address this issue.

APPENDIX

We aim to calculate a closed form solution for the perceived roll tilt angle as a function of the actual roll tilt angle and gravity level [$\theta_{per} = f(\theta, G)$]. As will be seen, this is only possible utilizing a numerical equation solver. However, for the case of static roll tilt we will provide the single equation, which can be solved numerically, reducing the complexity compared with the full dynamic simulation.

First, the perceived roll tilt angle, from simple geometry, is given as a function of the perceived direction of gravity:

$$\theta_{per} = \operatorname{atan}\left(\hat{g}_y / \hat{g}_z\right) \tag{A1}$$

Furthermore, we assumed the internal model of gravity requires its magnitude to be equal to 1 Earth G:

$$\hat{g}_y^2 + \hat{g}_z^2 = 1 \tag{A2}$$

For roll tilt with no linear acceleration, the applied GIF (f) is given by:

$$f_y = -G\sin(\theta),\ f_z = -G\cos(\theta) \tag{A3}$$

Given these inputs, assuming that the otolith dynamics and internal model of the otolith dynamics can be approximated by identity matrices, and solving for the upper loop of the Observer model yields the following two relationships:

$$\hat{\alpha}_y\left(1 - K_{a_u}\right) = \hat{g}_y + K_{a_u} G\sin(\theta) \tag{A4}$$

$$\hat{\alpha}_z\left(1 - K_{a_{u\perp}}\right) = \hat{g}_z + K_{a_{u\perp}} G\cos(\theta) \tag{A5}$$

Finally, the steady-state of static tilt implies that the error in the direction of perceived GIF is infinitesimally small:

$$\left|\hat{e}_f\right| = 0 = \operatorname{acos}\left(\frac{\vec{\alpha}_f}{\left|\vec{\alpha}_f\right|} \cdot \frac{\hat{\vec{\alpha}}_f}{\left|\hat{\vec{\alpha}}_f\right|}\right) \tag{A6}$$

With the applied GIF (f) in *Eq. A3* and the assumption that the otolith dynamics are unity, *Eq. A6* yields the following relationship:

$$\hat{\alpha}_{fy}^2 + \hat{\alpha}_{fz}^2 = \left(-\sin(\theta)\hat{\alpha}_{fy} - \cos(\theta)\hat{\alpha}_{fz}\right)^2 \tag{A7}$$

Combining *Eqs. A2*, *A4*, *A5*, and *A7* can yield the following relationship for $\theta \geq 0$, which contains only terms $\hat{g}_z$, θ, G, K_{a_u}, $K_{a_{u\perp}}$:

$$\begin{aligned} 0 = &\left[\frac{-1}{1 - K_{a_u}}\sqrt{1 - \hat{g}_z^2} + \frac{K_{a_u}}{1 - K_{a_u}} G\sin(\theta)\right]^2 \\ &+ \left[\frac{1}{1 - K_{a_{u\perp}}}\hat{g}_z + \frac{K_{a_{u\perp}}}{1 - K_{a_{u\perp}}} G\cos(\theta)\right]^2 \\ &- \left[-\sin(\theta)\left(\frac{-1}{1 - K_{a_u}}\sqrt{1 - \hat{g}_z^2} + \frac{K_{a_u}}{1 - K_{a_u}} G\sin(\theta)\right)\right. \\ &\left. - \cos(\theta)\left(\frac{1}{1 - K_{a_{u\perp}}}\hat{g}_z + \frac{K_{a_{u\perp}}}{1 - K_{a_{u\perp}}} G\cos(\theta)\right)\right]^2 \end{aligned} \tag{A8}$$

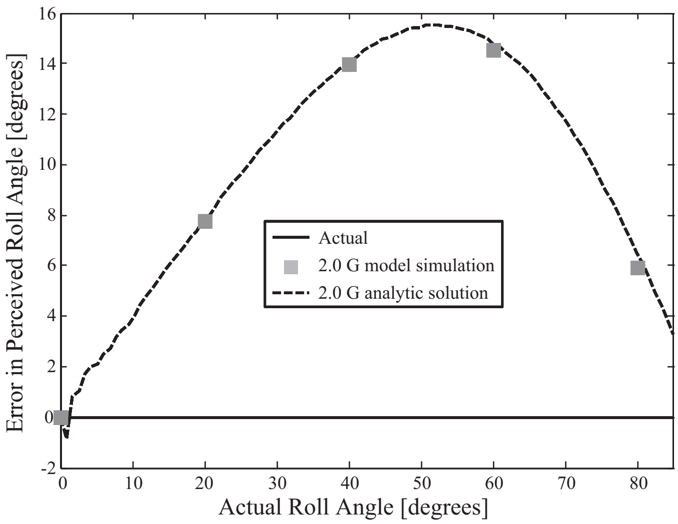

Fig. A1. Comparison of analytic solution to model simulation results. The model was simulated with a 0, 20, 40, 60, and 80° roll tilts in 2 Gs, yielding overestimation (grey squares). The analytic solution (see APPENDIX) with numerical maximization was solved at a range of angles (dotted black line) and compares well with the full dynamic simulation. In both the model simulation and the analytic solution $K_{a_u} = -2$.

Equation A8 cannot be analytically solved for a closed form solution, $\hat{g}_z = f(\theta, G, K_{a_u}, K_{a_{u\perp}})$. However, for a given condition (θ, G) and set of parameters $(K_{a_u}, K_{a_{u\perp}})$, *Eq. 8* can be solved numerically for $\hat{g}_z$. Specifically for $0 \leq \theta < 90°$, the right side of *Eq. 8* is ≤ 0, and at only one value of $\hat{g}_z$ does it equal or nearly approach 0, so we numerically find the value of $\hat{g}_z$, which maximizes the right-hand side of *Eq. A8*. Once $\hat{g}_z$ is determined, $\hat{g}_y$ is calculated from *Eq. A2*, and then finally the perceived roll tilt angle is calculated using *Eq. A1*. A comparison between the steady-state analytic solution and the dynamic Observer model simulation for static roll tilt perception at 2 Gs is given in Fig. A1, showing a near identical match.

ACKNOWLEDGMENTS

We appreciate the participation of our anonymous subjects. We thank Caglar Unlu and Ebubekir Tipi for technical support; Amer Makhleh and Gregory Kennedy for assistance in data collection; Alan Natapoff for advice on statistics; and Kevin Duda, Paul DiZio, Faisal Karmali, and our anonymous reviewers for reviewing a draft of this manuscript and helpful suggestions.

GRANTS

This work was supported by the National Space Biomedical Research Institute (NSBRI) through National Aeronautics and Space Administration Grant NCC9-58 (to T. K. Clark, C. M. Oman, and L. R. Young) and via National Institute of Deafness and Other Communications Disorders Grant R01-DC-04158 (to D. M. Merfeld). We also thank Bill Mitchell and NASTAR Center for additional project support.

DISCLOSURES

No conflicts of interest, financial or otherwise, are declared by the author(s).

AUTHOR CONTRIBUTIONS

Author contributions: T.K.C., M.C.N., C.M.O., D.M.M., and L.R.Y. conception and design of research; T.K.C. and M.C.N. performed experiments; T.K.C., M.C.N., C.M.O., D.M.M., and L.R.Y. analyzed data; T.K.C., M.C.N., C.M.O., D.M.M., and L.R.Y. interpreted results of experiments; T.K.C. prepared figures; T.K.C. drafted manuscript; T.K.C., M.C.N., C.M.O., D.M.M., and L.R.Y. edited and revised manuscript; T.K.C., M.C.N., C.M.O., D.M.M., and L.R.Y. approved final version of manuscript.

REFERENCES

Angelaki DE, McHenry MQ, Dickman JD, Newlands SD, Hess BJ. Computation of inertial motion: neural strategies to resolve ambiguous otolith information. *J Neurosci* 19: 316–327, 1999.

Aubert H. Eine scheinbare bedeutende drehung von objekten bei neigung des kopfes nach rechts oder links. *Arch Pathol Anat* 20: 381–393, 1861.

Barnett-Cowan M. Vestibular perception is slow: a review. *Multisens Res* 26: 387–403, 2013.

Barnett-Cowan M, Harris LR. Perceived self-orientation in allocentric and egocentric space: effects of visual and physical tilt on saccadic and tactile measures. *Brain Res* 1242: 231–243, 2008.

Barnett-Cowan M, Jenkin HL, Dyde RT, Jenkin MR, Harris LR. Asymmetrical representation of body orientation. *J Vis* 13: 3, 2013.

Bauermeister M, Werner H, Wapner S. The effect of body tilt on tactual-kinesthetic perception of verticality. *Am J Psychol* 77: 451–456, 1964.

Betts GA, Curthoys IS. Visually perceived vertical and visually perceived horizontal are not orthogonal. *Vision Res* 38: 1989–1999, 1998.

Borah J, Young LR. Orientation perception during aircraft coordinated turns. In: *AIAA 20th Aerospace Sciences Meeting*. Orlando, FL: American Institute of Aeronautics and Astronautics, 1982.

Borah J, Young LR, Curry RE. Optimal estimator model for human spatial orientation. *Ann NY Acad Sci* 545: 51–73, 1988.

Bortolami SB, Pierobon A, Dizio P, Lackner JR. Localization of the subjective vertical during roll, pitch, and recumbent yaw body tilt. *Exp Brain Res* 173: 364–373, 2006a.

Bortolami SB, Rocca S, Daros S, Dizio P, Lackner JR. Mechanisms of human static spatial orientation. *Exp Brain Res* 173: 374–388, 2006b.

Bos JE, Bles W. Motion sickness induced by optokinetic drums. *Aviat Space Environ Med* 75: 172–174, 2004.

Brown EL, Hecht H, Young LR. Sensorimotor aspects of high-speed artificial gravity: I. sensory conflict in vestibular adaptation. *J Vestib Res* 12: 271–282, 2002.

Chelette TL. Measuring the head tilt illusion during sustained acceleration. *Human Systems IAC Gateway* 12: 4–6, 2001.

Chelette TL, Martin EJ, Albery WB. The effect of head tilt on perception of self-orientation while in a greater than one G environment. *J Vestib Res* 5: 1–17, 1995.

Cheung CC, Hecht H, Jarchow T, Young LR. Threshold-based vestibular adaptation to cross-coupled canal stimulation. *J Vestib Res* 17: 171–181, 2007.

Cohen MM. Elevator illusion–influences of otolith organ activity and neck proprioception. *Percept Psychophys* 14: 401–406, 1973.

Colenbrander A. Eye and otoliths. *Aeromed Acta* 9: 45–91, 1963.

Correia MJ, Hixson WC, Niven JI. On predictive equations for subjective judgments of vertical and horizon in a force field. *Acta Otolaryngol Suppl* 230: 1–20, 1968.

Corvera J, Hallpike CS, Schuster EH. A new method for the anatomical reconstruction of the human macular planes. *Acta Otolayngol* 49: 4–16, 1958.

Curthoys IS, Betts GA, Burgess AM, MacDougall HG, Cartwright AD, Halmagyi GM. The planes of the utricular and saccular maculae of the guinea pig. *Ann NY Acad Sci* 871: 27–34, 1999.

Dai MJ, Curthoys IS, Halmagyi GM. A model of otolith stimulation. *Biol Cybern* 60: 185–194, 1989.

De Vrijer M, Medendorp WP, Van Gisbergen JA. Accuracy-precision trade-off in visual orientation constancy. *J Vis* 9: 1–15, 2009.

Dyde RT, Jenkin MR, Harris LR. The subjective visual vertical and the perceptual upright. *Exp Brain Res* 173: 612–622, 2006.

Dyde RT, Jenkin MR, Jenkin HL, Zacher JE, Harris LR. The effect of altered gravity states on the perception of orientation. *Exp Brain Res* 194: 647–660, 2009.

Edgerton VR, McCall GE, Hodgson JA, Gotto J, Goulet C, Fleischmann K, Roy RR. Sensorimotor adaptations to microgravity in humans. *J Exp Biol* 204: 3217–3224, 2001.

Fernandez C, Goldberg JM. Physiology of peripheral neurons innervating otolith organs of squirrel-monkey. II. Directional selectivity and force-response relations. *J Neurophysiol* 39: 985–995, 1976a.

Fernandez C, Goldberg JM. Physiology of peripheral neurons innervating otolith organs of the squirrel monkey. I. Response to static tilts and to long-duration centrifugation. *J Neurophysiol* 39: 970–984, 1976b.

Fernandez C, Goldberg JM. Physiology of peripheral neurons innervating otolith organs of the squirrel monkey. III. Response dynamics. *J Neurophysiol* 39: 996–1008, 1976c.

Garrick-Bethell I, Jarchow T, Hecht H, Young LR. Vestibular adaptation to centrifugation does not transfer across planes of head rotation. *J Vestib Res* 18: 25–37, 2008.

Gilson RD, Guedry FE, Hixson WC, Niven JI. Observations on perceived changes in aircraft attitude attending head movements made in a 2-g bank and turn. *Aerospace Med* 44: 90–92, 1973.

Glasauer S. Interaction of semicircular canals and otoliths in the processing structure of the subjective zenith. *Ann NY Acad Sci* 656: 847–849, 1992.

Glasauer S, Brandt T. Noncommutative updating of perceived self-orientation in three dimensions. *J Neurophysiol* 97: 2958–2964, 2007.

Glasauer S, Mittelstaedt H. Determinants of orientation in microgravity. *Acta Astronaut* 27: 1–9, 1992.

Goldberg JM, Fernandez C. Physiology of peripheral neurons innervating semicircular canals of squirrel monkey. I. Resting discharge and response to constant angular accelerations. *J Neurophysiol* 34: 635–660, 1971.

Golding JF. Motion sickness susceptibility questionnaire revised and its relationship to other forms of sickness. *Brain Res Bull* 47: 507–516, 1998.

Golding JF. Predicting individual differences in motion sickness susceptibility by questionnaire. *Person Individ Differ* 41: 237–248, 2006.

Gonshor A, Melvill Jones G. Plasticity in the adult human vestibuloocular reflex. *Arc Proc Can Fed Biol Soc* 14: 1971.

Goonetilleke SC, Mezey LE, Burgess AM, Curthoys IS. On the relation between ocular torsion and visual perception of line orientation. *Vision Res* 48: 1488–1496, 2008.

Graybiel A, Clark B, Zarriello JJ. Observations on human subjects living in a "slow rotating room" for periods of two days. *Arch Neurol* 3: 55–73, 1960.

Green AM, Angelaki DE. An integrative neural network for detecting inertial motion and head orientation. *J Neurophysiol* 92: 905–925, 2004.

Guedry FE, Montague EK. Quantitative evaluation of the vestibular coriolis reaction. *Aerospace Med* 32: 487–500, 1961.

Guedry FE, Rupert AH. Steady-state and transient G-excess effects. *Aviat Space Environ Med* 62: 252–253, 1991.

Guerraz M, Luyat M, Poquin D, Ohlmann T. The role of neck afferents in subjective orientation in the visual and tactile sensory modalities. *Acta Otolaryngol* 120: 735–738, 2000.

Haslwanter T, Jaeger R, Mayr S, Fetter M. Three-dimensional eye-movement responses to off-vertical axis rotations in humans. *Exp Brain Res* 134: 96–106, 2000.

Holly JE, Davis SM, Sullivan KE. Differences between perception and eye movements during complex motions. *J Vestib Res* 21: 193–208, 2011.

Holly JE, McCollum G. The shape of self-motion perception. 2. Framework and principles for simple and complex motion. *Neuroscience* 70: 487–513, 1996.

Jarchow T, Wirz M, Haslwanter T, Dietz V, Straumann D. Perceived horizontal body position in healthy and paraplegic subjects: effect of centrifugation. *J Neurophysiol* 90: 2973–2977, 2003.

Jarchow T, Young LR. Adaptation to head movements during short radius centrifugation. *Acta Astronaut* 61: 881–888, 2007.

Jia H, Yu L, Bi H, Wang K, Liu Z, Xie S. Perception of the cabin attitude changes in hypergravity. *Aviat Space Environ Med* 73: 191–193, 2002.

Kalman RE. A new approach to linear filtering and prediction problems. *J Basic Eng* 82D: 35–45, 1960.

Kalman RE, Bucy RS. New results in linear filtering and prediction problems. *J Basic Eng* 83D: 95–108, 1961.

Kaptein RG, Van Gisbergen JA. Canal and otolith contributions to visual orientation constancy during sinusoidal roll rotation. *J Neurophysiol* 95: 1936–1948, 2006.

Karmali F, Merfeld DM. A distributed, dynamic, parallel computational model: the role of noise in velocity storage. *J Neurophysiol* 108: 390–405, 2012.

Kornheiser AS. Adaptation to laterally displaced vision–review. *Psychol Bull* 83: 783–816, 1976.

Lackner JR, DiZio P. Motor control and learning in altered dynamic environments. *Curr Opin Neurobiol* 15: 653–659, 2005.

Lackner JR, DiZio PA. Adaptation to rotating artificial gravity environments. *J Vestib Res* 13: 321–330, 2003.

Laurens J, Droulez J. Bayesian processing of vestibular information. *Biol Cybern* 96: 389–404, 2007.

Luenburger DG. An introduction to observers. *IEEE Trans Automat Contr* 16: 596–602, 1971.

MacNeilage PR, Ganesan N, Angelaki DE. Computational approaches to spatial orientation: from transfer functions to dynamic bayesian inference. *J Neurophysiol* 100: 2981–2996, 2008.

Melville Jones G. Origin significance and amelioration of coriolis illusions from semicircular canals–a non-mathematical appraisal. *Aerospace Med* 41: 483–490, 1970.

Merfeld DM, Park S, Gianna-Poulin C, Black FO, Wood S. Vestibular perception and action employ qualitatively different mechanisms. I. Frequency response of VOR and perceptual responses during translation and tilt. *J Neurophysiol* 94: 186–198, 2005a.

Merfeld DM, Park S, Poulin CG, Black FO, Wood S. Vestibular perception and action employ qualitatively different mechanisms. II. VOR and perceptual responses during combined tilt & translation. *J Neurophysiol* 94: 199–205, 2005b.

Merfeld DM, Young LR, Oman CM, Shelhammer MJ. A multidimensional model of the effect of gravity on the spatial orientation of the monkey. *J Vestib Res* 3: 141–161, 1993.

Merfeld DM, Zupan L, Peterka RJ. Humans use internal models to estimate gravity and linear acceleration. *Nature* 398: 615–618, 1999.

Merfeld DM, Zupan LH. Neural processing of gravitoinertial cues in humans. III. Modeling tilt and translation responses. *J Neurophysiol* 87: 819–833, 2002.

Merfeld DM, Zupan LH, Gifford CA. Neural processing of gravito-inertial cues in humans. II. Influence of the semicircular canals during eccentric rotation. *J Neurophysiol* 85: 1648–1660, 2001.

Miller EF. Counterrolling of the human eyes produced by head tilt with respect to gravity. *Acta Otollaryngologica* 54: 479–501, 1962.

Miller EF, Graybiel A. Effect of gravitoinertial force on ocular counter-rolling. *J Appl Physiol* 31: 697–700, 1971.

Miller EF, Graybiel A. Magnitude of gravitoinertial force an independent variable in egocentric visual localization of horizontal. *J Exp Psychol* 71: 452–460, 1966.

Mittelstaedt H. A new solution to the problem of the subjective vertical. *Naturwissenschaften* 70: 272–281, 1983a.

Mittelstaedt H. The role of the pitched-up orientation of the otoliths in two recent models of the subjective vertical. *Biol Cybern* 61: 405–416, 1989.

Mittelstaedt H. The subjective vertical as a function of visual and extraretinal cues. *Acta Psychol (Amst)* 63: 63–85, 1986.

Mittelstaedt H. Towards understanding the flow of information between objective and subjective space. In: *Neuroethology and Behavioral Physiology*, edited by Huber F, Markl H. Berlin: Springer-Verlag, 1983b, p. 382–402.

Mittelstaedt H, Fricke E. The relative effect of saccular and somatosensory information on spatial perception and control. *Adv Otorhinolaryngol* 42: 24–30, 1988.

Muller GE. Uber das aubertsche phanomen. *Z Sinnesphysiol* 49: 109–246, 1916.

Newman MC. A multisensory observer model for human spatial orientation perception. In: *Aeronautics and Astronautics*. Cambridge, MA: MIT, 2009.

Nooij SA, Bos JE, Groen EL. Velocity storage activity is affected after sustained centrifugation: a relationship with spatial disorientation. *Exp Brain Res* 190: 165–177, 2008.

Oman CM. A heuristic mathematical-model for the dynamics of sensory conflict and motion sickness. *Acta Otolaryngol* 392: 1–44, 1982.

Oman CM. Motion sickness–a synthesis and evaluation of the sensory conflict theory. *Can J Physiol Pharmacol* 68: 294–303, 1990.

Oman CM. Sensory conflict in motion sickness: an observer theory approach. In: *Pictorial Communication in Virtual and Real Environments*, edited by Ellis SR, Kaiser MK, Grunwald A. London: Taylor & Francis, 1991, p. 362–367.

Oman CM, Bock OL, Huang JK. Visually induced self-motion sensation adapts rapidly to left-right visual reversal. *Science* 209: 706–708, 1980.

Oman CM, Lichtenberg BK, Money KE, Mccoy RK. MIT Canadian vestibular experiments on the Spacelab-1 Mission: 4. Space motion sickness–symptoms, stimuli, and predictability. *Exp Brain Res* 64: 316–334, 1986.

Ormsby CC, Young LR. Perception of static orientation in a constant gravito-inertial environment. *Aviat Space Environ Med* 47: 159–164, 1976.

Park S, Gianna-Poulin C, Black FO, Wood S, Merfeld DM. Roll rotation cues influence roll tilt perception assayed using a somatosensory technique. *J Neurophysiol* 96: 486–491, 2006.

Pettorossi VE, Panichi R, Botti FM, Kyriakareli A, Ferraresi A, Faralli M, Schieppati M, Bronstein AM. Prolonged asymmetric vestibular stimulation induces opposite, long-term effects on self-motion perception and ocular responses. *J Physiol* 591: 1907–1920, 2013.

Rader AA. Motion perception with conflicting or congruent visual and vestibular cues. In: *Aeronautics and Astronautics*. Cambridge, MA: MIT, 2009.
Rader AA, Oman CM, Merfeld DM. Motion perception during variable-radius swing motion in darkness. *J Neurophysiol* 102: 2232–2244, 2009.
Rader AA, Oman CM, Merfeld DM. Perceived tilt and translation during varianble-radius swing motion with congruent or conflicting visual and vestibular cues. *Exp Brain Res* 210: 173–184, 2011.
Reason JT. Motion sickness adaptation–neural mismatch model. *J R Soc Med* 71: 819–829, 1978.
Reason JT, Benson AJ. Voluntary movement control and adaptation to cross-coupled stimulation. *Aviat Space Environ Med* 49: 1275–1280, 1978.
Schöne H. On the role of gravity in human spatial orientation. *Aerospace Med* 35: 764–772, 1964.
Schöne H, Parker DE. Inversion of the effect of increased gravity on the subjective vertical. *Naturwissenschaften* 54: 288–289, 1967.
Schöne H, Parker DE, Mortag HG. Subjective vertical as a function of body position and gravity magnitude. *Natrwissenschaften* 54: 288, 1967.
Schuler JR, Bockisch CJ, Straumann D, Tarnutzer AA. Precision and accuracy of the subjective haptic vertical in the roll plane. *BMC Neurosci* 11: 83, 2010.
Seidler RD. Differential transfer processes in incremental visuomotor adaptation. *Motor Control* 9: 40–58, 2005.
Selva P. Modeling of the vestibular system and nonlinear models for human spatial orientation perception. In: *I'Institut superieur de l'Aeronautique et de l'Espace*. Toulouse, France: L'Universite de Toulouse, 2009.
Selva P, Oman CM. Relationships between Observer and Kalman Filter models for human dynamic spatial orientation. *J Vestib Res* 22: 69–80, 2012.
Tribukait A, Eiken O. Flight experience and the perception of pitch angular displacements in a gondola centrifuge. *Aviat Space Environ Med* 83: 496–503, 2012.
Tribukait A, Eiken O. Roll-tilt perception during gondola centrifugation: influence of steady-state acceleration (G) level. *Aviat Space Environ Med* 77: 695–703, 2006a.
Tribukait A, Eiken O. Semicircular canal contribution to the perception of roll tilt during gondola centrifugation. *Aviat Space Environ Med* 76: 940–946, 2005.
Tribukait A, Eiken O. Semicircular canal influence on the visually perceived eye level during gondola centrifugation. *Aviat Space Environ Med* 77: 500–508, 2006b.
Valko Y, Lewis RF, Priesol AJ, Merfeld DM. Vestibular labyrinth contributions to human whole-body motion discrimination. *J Neurosci* 32: 13537–13542, 2012.
van Beuzekom AD, van Gisbergen JA. Properties of the internal representation of gravity inferred from spatial-direction and body-tilt estimates. *J Neurophysiol* 84: 11–27, 2000.
Vingerhoets RA, De Vrijer M, Van Gisbergen JA, Medendorp WP. Fusion of visual and vestibular tilt cues in the perception of visual vertical. *J Neurophysiol* 101: 1321–1333, 2009.
Vingerhoets RA, Medendorp WP, Van Gisbergen JA. Body-tilt and visual verticality perception during multiple cycles of roll rotation. *J Neurophysiol* 99: 2264–2280, 2008.
Vingerhoets RA, Van Gisbergen JA, Medendorp WP. Verticality perception during off-vertical axis rotation. *J Neurophysiol* 97: 3256–3268, 2007.
Wade SW, Curthoys IS. The effect of ocular torsional position on perception of the roll-tilt of visual stimuli. *Vision Res* 37: 1071–1078, 1997.
Welch RB, Bridgeman B, Williams JA, Semmler R. Dual adaptation and adaptive generalization of the human vestibulo-ocular reflex. *Percept Psychophys* 60: 1415–1425, 1998.
Wertheim AH, Mesland BS, Bles W. Cognitive suppression of tilt sensations during linear horizontal self-motion in the dark. *Perception* 30: 733–741, 2001.
Woellner RC, Graybiel A. Counterrolling of the eyes and its dependence on the magnitude of gravitational or inertial force acting laterally on the body. *J Appl Physiol* 14: 632–634, 1959.
Young LR, Hecht H, Lyne LE, Sienko KH, Cheung CC, Kavelaars J. Artificial gravity: head movements during short-radius centrifugation. *Acta Astronaut* 49: 215–226, 2001.
Young LR, Sienko KH, Lyne LE, Hecht H, Natapoff A. Adaptation of the vestibulo-ocular reflex, subjective tilt, and motion sickness to head movements during short-radius centrifugation. *J Vestib* 13: 65–77, 2003.
Zupan LH, Merfeld DM. Neural processing of gravito-inertial cues in humans. IV. Influence of visual rotational cues during roll optokinetic stimuli. *J Neurophysiol* 89: 390–400, 2003.
Zupan LH, Merfeld DM, Darlot C. Using sensory weighting to model the influence of canal, otolith and visual cues on spatial orientation and eye movements. *Biol Cybern* 86: 209–230, 2002.
Zupan LH, Peterka RJ, Merfeld DM. Neural processing of gravito-inertial cues in humans. I. Influence of the semicircular canals following post-rotatory tilt. *J Neurophysiol* 84: 2001–2015, 2000.